MAGNETIC MATERIALS, BULK

1. Introduction

All materials that are magnetized by, ie, exhibit a response in, a magnetic field are magnetic materials. Magnetism is classified according to the nature of the magnetic response, ie, diamagnetism, paramagnetism, ferromagnetism, antiferromagnetism, ferrimagnetism, metamagnetism, parasitic ferromagnetism, and mictomagnetism (spin glass). Although the observed response to an applied field is the same for ferromagnetism and ferrimagnetism, there is a distinct difference in the microscopic–atomistic source of the observed magnetic behavior. In a fully magnetized ferromagnet, the atomic–ion moments are all aligned in the same direction. This is not so for a ferrimagnet and hence the magnitude of the observed bulk magnetization is smaller. The extreme case of zero magnetization is called antiferromagnetic behavior. Most commercially important magnetic materials are ferromagnets and ferrimagnets (see also FERRITES).

2. Theory

2.1. Types of Magnetism. The two atomic origins of magnetism are the spin and orbital motions of electrons. Diamagnetism occurs when the orbital rotation of the electrons is induced electromagnetically by an applied field. This weak magnetism is characterized by magnetization that is directed opposite to the applied field. The susceptibility $\kappa = M/H$, where M is the magnetization and H is the magnetic-field strength, is ca 10^{-5} and, with few exceptions, is independent of temperature. Many metals and most nonmetals are diamagnetic. These substances usually contain electrons that constitute a closed shell such that the atom as a whole has no permanent magnetic moment.

In paramagnetism, the magnetization is aligned parallel to the applied field and the susceptibility is 10^{-3} to 10^{-5}. Most paramagnetic materials contain atoms or ions that have a permanent magnetic moment but which are unaligned except in the presence of an applied field. In the latter case, the susceptibility is independent of the applied field and is inversely proportional to the temperature; examples include many salts of the iron and rare-earth families, platinum and palladium metals, and ferromagnetic materials when these are above their Curie point. Conduction electrons, which form an energy band in metals, exhibit a Pauli paramagnetism the susceptibility of which is independent of temperature. Thus, in some substances, eg, the alkali metals and metals such as copper [7440-50-8] (qv), silver [7440-22-4], and gold [7440-57-5], both diamagnetism and Pauli paramagnetism exist and the net value of susceptibility depends on the difference of two comparable quantities. Susceptibility is positive for the alkali metals and negative for Cu, Ag, and Au.

Where the permanent magnetic moments are aligned as a result of a strong positive interaction among neighboring atoms or ions, the material exhibits a spontaneous magnetization and ferromagnetism results. Examples include iron [7439-89-6] (qv), nickel [7440-02-0], cobalt [7440-48-4], and their alloys as well as many of the rare-earth elements (see LANTHANIDES). The principal source of

magnetism in Fe, Ni, and Co is the spin motion of the electrons, whereas orbital motion contributes substantially to the magnetism of the rare earths.

In the case where the permanent magnetic moments are aligned antiparallel as a result of a strong negative interaction, the complete cancellation of the neighboring atomic moments results in zero net magnetization called antiferromagnetism. Examples include chromium [7440-47-3], manganese [7439-96-9], manganese(II) oxide [1344-43-0], MnO, and nickel oxide [1313-99-1], NiO. In compounds containing two or more kinds of atoms or ions that exhibit different values of magnetic moment, the cancellation is incomplete. The result is a net value of magnetization, as in the case of ferromagnetism. Such incomplete antiferromagnetism is called ferrimagnetism and is exemplified by the ferrites (qv), metal oxides that have a spinel structure.

Metamagnetism refers to the appearance of a net magnetization resulting from a transition from antiferromagnetism to ferromagnetism by the application of a strong field or by a change of temperature. Manganese diauride [12006-65-4], $MnAu_2$ and iron(II) chloride [7758-94-3], $FeCl_2$, undergo the transition by field application, and heavy rare-earth metals, eg, terbium [7440-27-9], dysprosium [7429-91-6], and holmium [7440-60-0], undergo the transition by temperature change.

Parasitic ferromagnetism is a weak ferromagnetism that accompanies antiferromagnetism, eg, in α-ferric oxide [1309-37-1], α-Fe_2O_3. Possible causes include the presence of a small amount of ferromagnetic impurities, defects in the crystal, and slight deviations in the directions of the plus and minus spins from the original common axis.

Mictomagnetism, or spin glass, refers to the onset of short-range magnetic order in alloys that have spin orientations which are frozen at a critical low temperature. In contrast to ferromagnetism and antiferromagnetism, however, this magnetic order is not long range. Spin glass is associated with a cusp in the susceptibility at a critical temperature and generally occurs in alloys containing a small fraction of magnetic atoms embedded in a nonmagnetic matrix, eg, copper manganese (1:1) [12272-98-9], CuMn, or gold ferride (1:1) [12399-92-2], AuFe. Mictomagnetic behavior, however, includes other features, eg, field cooling effects, such as displacements of the magnetization curve from zero field, and occurs in more concentrated alloys where incidences of structural clusters of near-neighbor magnetic atoms are high (1,2).

2.2. Magnetic Domains. Magnetic domains are associated with ferromagnetic, antiferromagnetic, or ferrimagnetic solids. In the demagnetized condition, these materials do not possess a net magnetization in the bulk because there are domains, ie, local regions within which the magnetic moments of all atoms are aligned. The direction of these moments, however, changes from one domain to another such that the net magnetization is zero for the solid. The transition region between domains is the domain wall or boundary and is a region of high energy. Typical domain sizes are 10^{-1} to 10^{-5} cm and domain-wall thicknesses are ca 100 nm for Fe. Domains arise as a result of minimizing a total energy composed of three principal contributions. The exchange energy tends to align all magnetic moments in one direction which maximizes the magnetostatic energy. This energy can be reduced by subdividing the solid into domains. The direction of alignment of the magnetic moments inside each domain,

however, is not arbitrary. Instead, alignment is directed along an easy axis, a direction of minimum anisotropy energy.

2.3. Magnetic Anisotropy Energy. There are several kinds of magnetic anisotropy energy and perhaps the most well known is the magnetocrystalline anisotropy. Only a crystalline solid has this property because the energy is dictated by the symmetry of the crystal lattice. For example, in bcc Fe, the easy axis is in a $\langle 100 \rangle$ direction and in fcc Ni, it is in a $\langle 111 \rangle$ direction.

Another kind of magnetic anisotropy is magnetostrictive anisotropy, through which the magnetic moments tend to respond to the application of a stress. Conversely, a change in dimension of the material accompanies the application of an applied field. If the alignment is parallel to a tensile-stress axis, the material has positive magnetostriction; if the alignment is perpendicular, the material has negative magnetostriction. Nickel is an example of the latter.

Shape anisotropy is related to the magnetostatic energy of a magnet. A needle-shaped sample tends to line the atomic moments along the needle axis and a disk-shaped sample tends to line these moments parallel to the disk surface.

Thermomagnetic anisotropy, also referred to as induced anisotropy or magnetic annealing anisotropy, is a uniaxial anisotropy that is developed in some materials, primarily alloys, by heat treating below the Curie temperature in the presence of a magnetic field. The origin is thought to be a short-range directional ordering of the nearest neighboring atom pairs (3).

Some materials that are atomically ordered also develop a slip-induced anisotropy as a result of plastic deformation. The origin is thought to be identical to that of thermomagnetic anisotropy, ie, short-range directional order, except that the order is brought on by deformation rather than by heat treatment in a field (3,4).

Magnetostrictive, shape, and thermomagnetic anisotropies are not properties solely of the crystalline lattice and, therefore, also can be manifested in amorphous materials. The mechanism of slip-induced anisotropy requires the existence of atomic ordering (long- or short-ranged) and, hence, a crystalline structure. In alloys such as silicon steel for transformer applications, magnetocrystalline energy predominates. In alloys such as the permalloys (Ni–Fe-based), several kinds of anisotropy energy can dominate depending on the work history and thermal treatment of the material.

2.4. Technical Magnetic Behavior. When a magnetic-field strength H is applied to a ferromagnetic or ferrimagnetic material, the latter develops a flux density or induction B as a result of orientation of the magnetic domains. The relation between B and H is

$$B = \mu_0(H + M) = \mu_0 H + J$$

where B, the number of lines of magnetic flux per unit of cross-sectional area, is in T ($= 1.0 \times 10^{-4}$ G) or Wb/m^2; H is in A/m ($=$ Oe/79.58); M, the magnetization, is in A/m; and μ_0, the permeability of free space, is a constant equal to $4\pi \times 10^{-7}$ $(T \cdot m)/A$ (1.0 G/Oe). The product $\mu_0 M$ is the magnetic polarization and is given in T, and generally is denoted by J. Discussions and recommendations regarding these systems are available (5–8).

A plot of induction vs field strength for an initially demagnetized material is shown in Figure 1. The curve is interpreted in terms of rearrangement of the domain structure. In the demagnetized state, the magnetizations of various domains are oriented randomly so that there is no net magnetization for the sample. When a small field is applied, domains that are favorably oriented, with respect to the field direction, grow at the expense of the unfavorable domains by the reversible motion of domain walls away from pinning points, eg, inclusions and grain boundaries. This motion results in a small rise in induction. At higher fields, the induction rises rapidly as the motion becomes irreversible when the walls break loose from their pinning points. Each grain then consists of a single domain with its magnetization directed along the local easy axis, which is dictated by the anisotropy energy, nearly parallel to H. At higher fields, the local magnetization rotates reversibly into the direction of H. The induction increases very slowly as the polarization reaches its saturation value J_s, also referred to as M_s, the saturation magnetization, which is an intrinsic characteristic of the material. For soft magnetic materials, J_s is reached at low fields, in which case the value of saturation induction B_s is practically equal to J_s.

As the applied field is reduced, the induction does not retrace curve 1 but follows curve 2 as the domains at first merely rotate back to the nearest local easy axis direction. The value of B at $H = 0$ is B_r, the remanent induction. At $H = -H_c$, which is the coercive-field strength of coercive force or coercivity, the induction is zero. Upon increase of field, the induction follows curve 3, completing the hysteresis loop. Commercial magnetic materials generally are classified into soft magnets, where $H_c \leq 10$ A/cm (12.6 Oe), and hard or permanent magnets, where $H_c \geq 100$ A/cm (126 Oe). A number of applications also make use of semihard magnets in which 10 A/cm $< H_c <$ 100 A/cm.

For permanent-magnet materials where the coercivity is large, the demagnetization curve, which corresponds to the second quadrant of the hysteresis loop, sometimes is plotted as the polarization $J(= B - \mu_0 H)$ vs $H(B - H$ vs H) to show the intrinsic characteristics of the material. The value of H, for which $J = 0$, is the intrinsic coercivity H_{cJ}, whereas the usual coercivity, for which $B = 0$, is denoted by H_{cB} or H_c. For permanent magnets, the value $(BH)_{\max}$, the maximum energy product, is an important measure of quality. The value $(BH)_{\max}$, indicated in the second quadrant of Figure 1, represents the point of maximum efficiency where a given amount of magnetic flux is produced by the smallest amount of material.

The permeability $\mu = B/H$ is important information for soft magnetic materials. The most often quoted values are the initial permeability μ_i and the maximum permeability μ_m. These correspond to the initial and maximum slopes of the virgin magnetization curve, respectively (Fig. 1). Because the value of μ_i at $B/H = 0$ needs to be extrapolated from measurements at finite H, the value often is quoted in commercial catalogues at specific B or H. The quoted values usually are relative to the free-space value μ_0.

Other forms of permeability often are quoted as related to specific applications (9). A term closely related to the permeability is the volume susceptibility $\kappa = M/H$ which particularly characterizes diamagnetic and paramagnetic substances. A variety of definitions of susceptibilities is given in Reference 5.

When a ferromagnetic or ferrimagnetic substance is heated, the value of saturation polarization J_s decreases with temperature and reaches a zero value at the Curie temperature T_C or Curie point. Above this temperature, the material becomes paramagnetic because the magnetic moments of the atoms are prevented by thermal agitation from spontaneous alignment. The equivalent temperature for the transition from antiferromagnetism to paramagnetism is the Néel temperature.

3. Soft Magnetic Materials

Soft magnetic materials are characterized by high permeability and low coercivity. There are six principal groups of commercially important soft magnetic materials: iron and low carbon steels, iron–silicon alloys, iron–aluminum and iron–aluminum–silicon alloys, nickel–iron alloys, iron–cobalt alloys, and ferrites. In addition, iron–boron-based amorphous soft magnetic alloys are commercially available. Some have properties similar to the best grades of the permalloys whereas others exhibit core losses substantially below those of the oriented silicon steels. Table 1 summarizes the properties of some of these materials.

3.1. Iron and Low Carbon Steel. Research-grade (99.99+% pure) iron (qv) generally is obtained by zone refining (qv) or electrodeposition from high purity salts; total metallic and nonmetallic impurity levels are as low as 10–20 ppm. Such purity generally is too expensive for commercial use. Commercially pure iron, often referred to as Armco iron or magnetic ingot iron, is 99.9% pure. The chief impurity is oxygen (0.15 wt%) which is tied up as oxide inclusions and which does not greatly affect the magnetic properties. Typical magnetic properties of annealed sheet which has been prepared from magnetic ingot iron are shown in Table 1 (10) and Figure 2. The annealing is carried out at about 800°C. The carbon and nitrogen that are dissolved in the lattice at this temperature can precipitate at low temperature, causing magnetic aging which is manifested by a rise in coercivity. Nitrogen, in particular, precipitates slowly at room temperature, but the aging can be hastened by a heat treatment at ca 100°C which stabilizes the material.

Another way of stabilizing the iron is to add elements, eg, titanium and aluminum, to tie up the carbon and nitrogen in stable compounds. This type of iron is known as electromagnet iron and its magnetic properties are shown in Table 1. The magnetic properties of both types of commercially pure iron are nearly equivalent. The electromagnet iron has a somewhat larger resistivity and smaller coercivity. Iron having exceptionally low coercivity and high permeability can be prepared by careful annealing in pure H_2 at temperatures above 1300°C.

Low carbon steel for use as soft magnetic material contains <0.10 wt% C. It is considerably less expensive than the Si–Fe alloys and has reasonably good magnetic properties after decarburization. Therefore, it is widely used in low or intermittent duty motors where cost is of primary importance and loss is secondary. Typical magnetic properties of decarburized, low carbon steel sheets are shown in Table 1. Decarburization generally is carried out at ca 800°C in a suitable decarburizing atmosphere, eg, wet hydrogen. The carbon level can be lowered to 0.002–0.005% to decrease coercivity. The presence and distribution of the

insoluble carbon influences coercivity. For example, the coercivity of an SAE 1010 steel having a fine lamellar cementite, ie, Fe_3C, structure can be reduced by one half by a spherodization annealing at 680°C (11).

Commercial low carbon sheet steels for electrical applications are furnished in one of four grades according to the American Iron and Steel Institute (AISI) (12): cold-rolled lamination steel, type 1, ie, low grade material furnished to a controlled chemical composition in C, Mn, and P, which may be full-hard or annealed; cold-rolled lamination steel, type 2, ie, intermediate-grade material having magnetic properties improved by special mill processing; cold-rolled lamination steel, type 2S, ie, high grade material having guaranteed core-loss limits as referred to material decarburized to ca 0.005% C at 788°C for 1 h; and hot-rolled sheet steel which is used primarily for d-c applications and used as a low cost substitute for Armco iron.

3.2. Iron–Silicon Alloys. Iron–silicon alloys, commercially known as silicon steel, contain silicon up to about 4%. The addition of silicon to iron results in several beneficial effects: (*1*) silicon increases the electrical resistivity, thereby reducing the eddy-current loss and enhancing the a-c use of the alloy. This increase, together with the changes in some magnetic properties, is illustrated in Figure 3 (10). A fairly good approximation (13) relating the silicon content and resistivity in $\mu\Omega \cdot$ cm in commercial alloys is $\rho = 13.25 + 11.3(\%\ \text{Si})$. (*2*) Because Si reduces the size of the γ loop (fcc-phase field), high temperature heat treatment for purification and orientation control is possible without the deleterious effect of the α- γ-phase transformation. (*3*) Si decreases the value of the magnetocrystalline anisotropy energy K_1 (Fig. 3) and thus tends to enhance the permeability and to decrease the core loss. The decrease of the magnetostriction γ toward zero near 6% Si is particularly attractive in terms of lower core loss and transformer noise. However, the brittleness of alloys beyond about 4% Si has precluded utilization of such high silicon content.

The detrimental effects of Si addition are (*1*) Si increases the yield strength and decreases the ductility of iron such that commercial-grade materials are limited to ca 4% Si, and (*2*) as shown in Figure 3, the saturation induction and Curie temperature are decreased with increasing silicon content.

Silicon steel is used primarily at 60 or 50 Hz; thus the most important quality factor is core loss at a given induction level. Core loss has been improving. From 1900–1930, the improvement primarily resulted from advances in the art of steelmaking and processing. In 1934, the {110} ⟨001⟩ or cube-on-edge (COE) grain-oriented material was developed through a combination of cold work and recrystallization (14). In COE-oriented material a majority of grains have a {110} plane parallel to the sheet surface and a ⟨001⟩ direction parallel to the rolling direction. Because ⟨001⟩ is an easy axis for Si–Fe alloys, the domains are favorably oriented for high permeability and low loss when a field is applied in the rolling direction of the grain-oriented material. Guaranteed core-loss limits were critically specified at 1.5 T (1.5×10^4 G). Developments in manufacturing technology, eg, basic oxygen and electric furnaces for melting and refining and continuous hot and cold rolling of sheet stock using improved gauge and flatness control, have contributed to continuing improvements. Typical magnetic properties of nonoriented (M36 and M22) and 3.2% Si-oriented material (M6) are given in Table 1 and in Figure 2.

Grades of high induction, low loss material of exceptionally sharp COE orientation were introduced commercially in 1968 (15). As a result, core-loss guarantees are quoted at 1.7 T (1.7×10^4 G). Values of core loss of these new high induction grades along with conventional oriented grades are given in Table 2.

The development of a sharp COE texture in the finished strip requires complex control of numerous variables. The conventional commercial process (18) involves hot-rolling a cast ingot at ca 1370°C to a thickness of about 2 mm, annealing at 800–1000°C, and then cold-rolling to a final thickness of 0.27–0.35 mm in two steps of 70 and 50%, respectively, with a recrystallization (800–1000°C) anneal in between. The cold-rolled strip is decarburized (800°C) to ca 0.003% C in mixtures of wet H_2 and N_2, a step which also results in a primary recrystallized structure containing grains of the COE orientation. It is finally box-annealed (1200°C) in dry hydrogen to form the COE texture by secondary recrystallization, ie, the growth of the COE-oriented grains at the expense of their neighbors. A very important concept in the development of the secondary recrystallized COE structure involves grain-growth inhibitors. In the conventional process, manganese and sulfur, which occur naturally in steelmaking, form manganese(II) sulfide, MnS, inclusions. These inclusions retard the motion of grain boundaries during primary recrystallization. At the secondary recrystallization step, which takes place at a higher temperature, the inclusions are dissolved, allowing the preferential growth of the COE-oriented grains.

The Nippon Steel HI-B process (18) differs from the conventional process in the use of aluminum nitride [24304-00-5], AlN, in addition to MnS as a grain-growth inhibitor and a one-stage cold reduction of large deformation. A large cold reduction results in a sharper COE texture in the final strip, although it also enhances the undesirable growth of the primary grains. However, AlN is a more potent grain-growth inhibitor than MnS, permitting greater cold reduction without undesirable primary grain growth.

In the Kawasaki Steel RG-H process (18), antimony is added with manganese selenide, MnSe, or MnS as a grain-growth inhibitor. It is thought that Sb inhibits primary grain growth by segregating to the grain boundaries and acts in addition to the role of inclusions from MnSe or MnS. The RG-H process also introduced a two-step box-annealing, ie, a low temperature, long-time annealing (820–900°C, 5–50 h), followed by the usual high temperature (1200°C) purification. The COE temperature becomes sharper if the secondary recrystallization is conducted first at the low temperature. Finally, a low thermal expansion inorganic phosphate coating has been developed to impart a large tensile stress to the finished strip. Losses are reduced in the presence of a tensile stress.

In the General Electric–Allegheny Ludlum (GE–AL) process (18), boron and nitrogen with sulfur or selenium are used as grain-growth inhibitors. It is thought that controlled amounts of B, N, and S or Se in solute form segregate to the grain boundaries; hence, inclusions are not involved.

Core-Loss Limits. In the United States, flat-rolled, electrical steel is available in the following classes (12): nonoriented, fully processed; nonoriented, semiprocessed; nonoriented, full-hard; and grain-oriented, fully processed. Loss limits are quoted at 1.5 T (1.5×10^4 G). The loss limits at 1.7 T (1.7×10^4 G) of the fourth class and of the high induction grades are shown in Table 2. Typical

applications include use for transformers, generators, stators, motors, ballasts, and relays.

3.3. Iron–Aluminum and Iron–Aluminum–Silicon Alloys. The influence of aluminum on the physical and magnetic properties of iron is similar to that of silicon, ie, stabilization of the bcc phase, increased resistivity, decreased ductility, and decreased saturation magnetization, magnetocrystalline anisotropy, and magnetostriction. Whereas Si–Fe alloys are well established for electrical applications, the aluminum–iron alloys have not been studied commercially. However, small (up to ca 0.3%) amounts of Al have been added to the nonoriented grades of silicon steel, because the decrease in ductility is less with Al than with Si.

In the Fe–Al–Si ternary system, alloys close to the 9.5 Si, 5.6 Al composition exhibit very low magnetostriction and anisotropy. As a result, these show very high values of initial and maximum permeability. However, the ternary alloys are very brittle, a factor which limits their general usefulness.

A 16 wt% Al alloy (Alfernol, Vacodur 16) and the 9.5 wt% Si–5.6 wt% Al alloy (Sendust [12606-95-0]) are produced commercially. Their primary use is as recording-head material because of high hardness and high resistivity together with reasonably good permeability (see INFORMATION STORAGE MATERIALS). Typical property values of various recording-head materials are listed in Table 3. Both Sendust and ferrite generally are prepared by powder technology, although precision casting of Sendust and the use of ferrite single crystal also are being carried out commercially (see METALLURGY, POWDER).

3.4. Nickel–Iron Alloys. The Ni–Fe alloys in the permalloy range, from ca 35–90% Ni, probably are the most versatile soft magnetic alloys in use (see NICKEL AND NICKEL ALLOYS). Using suitable alloying additions and proper processing, the magnetic properties can be controlled within wide limits. Some exhibit high up to 100,000 μ_0 (9.274×10^{-19} J/T) initial permeability and are ideal for high quality electronic transformers and for magnetic shielding. Others display a square hysteresis loop shape, desirable in inverters, converters, and other saturable reactors. Still others show low remanence combined with the constant permeability needed for unbiased unipolar pulse transformers.

For alloys that usually are cooled from high temperature to room temperature, the fcc γ-phase exists from ca 30–100% Ni. In the low nickel regime, the γ-phase undergoes a martensitic transformation to the bcc α-phase with considerable hysteresis. Of prime importance to the magnetic behavior, however, is the appearance of the long-range-ordered Cu_3Au-type $L1_2$ structure near the Ni_3Fe composition below ca 500°C. The principal magnetic parameters in the Ni–Fe system are illustrated in Figure 4. The most pronounced effect of the $L1_2$ ordering is a large change in the value of K_1, making it less positive or more negative as indicated by the dashed slowly cooled curve in Figure 4. The highest initial permeability in the Ni–Fe system occurs in the 78.5% Ni alloy, but rapid cooling below 600°C is necessary. Magnetic theory indicates that high permeability is achieved by minimizing K_1 and λ_s. This occurs for the 78.5% Ni alloy in the quenched condition. If the alloy is cooled slowly, ordering sets in, K_1 becomes highly negative, and the permeability is degraded severely. With the addition of molybdenum, the kinetics of ordering is slowed and simultaneous attainment of zero K_1 and λ_s is possible with moderate cooling. In this

way, alloys of ca 4 wt% Mo and 79 wt% Ni reach very high values of permeability. The addition of molybdenum also has the beneficial effect of increased resistivity (lower eddy-current loss) but at the expense of lower saturation induction and Curie temperature.

In addition to magnetocrystalline anisotropy and magnetostriction, two other sources of magnetic anisotropy are important for Ni–Fe alloys. One is thermomagnetic anisotropy, which occurs when the material is annealed below its Curie temperature. Alloys near 60 wt% Ni where the Curie temperature is high (Fig. 4) are particularly responsive to magnetic annealing. This squares up the hysteresis loop in the field direction and conversely produces a skewed or flat loop of low remanence and constant permeability perpendicular to the field direction. The other source of anisotropy is slip-induced anisotropy, which is obtained by plastic deformation, eg, rolling or wire drawing. The effect is most pronounced when the material is atomically ordered prior to the deformation and also is manifested in a change in the shape of the hysteresis loop, although in a more complicated manner than by magnetic annealing. For Ni–Fe alloys, the thermomagnetic anisotropy energy is ca 0.1 kJ/m^3 (ca 10^3 erg/cm^3) and the slip-induced anisotropy energy is ca 10 kJ/m^3 (ca 10^5 erg/cm^3) both overlapping the values of K_1 and λ_s. The richness of anisotropy energies of the Ni–Fe alloys permits custom tailoring of engineering magnetic properties through control of chemistry and processing.

The magnetic and physical properties of some commercial Ni–Fe alloys are compared to those of other iron alloys in Table 4 and Figure 2. The alloys are grouped into three types: high initial permeability, square-loop, and skewed or flat-loop alloys. The alloys generally are used in sheet form as laminations, cut-cores, and tape-wound (toroidal) cores. Laminations usually are 0.35 and 0.15 mm thick for operations of 60–400 Hz, whereas tape cores generally are wound from thin-gauge material ranging from 0.025 to 0.10 mm thick to enable operating frequencies up to ca 25 kHz for the 0.025-mm material of the 4-79 Mo–Permalloy type. Tape-wound cores generally are made from strips 0.025, 0.050, and 0.10 mm thick, although miniature bobbin cores made from material 0.003–0.025 mm thick are available for operations to 500 kHz.

High Permeability Alloys. In the United States, initial permeability μ_i values generally are given as μ_{40}, measured at $B = 4$ mT (40 G) and 60 Hz for 0.35-mm thick material. In Europe, μ_4, measured at $H = 4$ mA/cm (5 mOe) and 50 Hz for 0.1-mm thick material generally is used. All values of μ_i are in units of μ_0.

Two broad classes of alloys have been developed. One is ca 50% Ni and is characterized by moderate permeability ($\mu_{40} =$ ca $10,000$) and high saturation ($B_s =$ ca 1.5 T (1.5×10^4 G)). The other is near 79% Ni and is characterized by high permeability ($\mu_{40} =$ ca $50,000$) but lower saturation ($B_s =$ ca 0.8 T (0.8×10^4 G)). A few suppliers also offer alloys of ca 36 wt% Ni, which have lower permeability than 50 wt% Ni but higher resistivity and lower cost. However, a 2% Mo, 34.5% Ni alloy exhibits a remarkable permeability μ_4 of 55,000 and a large resistivity of 90 $\mu\Omega \cdot$ cm (21).

The 50% Ni alloys generally range from 45–50 wt% Ni and may contain up to 0.5 wt% Mn and 0.35 wt% Si. The carbon level generally is kept below 0.03 wt%. Most alloys contain 48 wt% Ni, and some are available in two grades:

rotor grade, μ_{40} = ca 6000, useful for rotors and stators in which the magnetic properties must be nondirectional; and transformer grade, μ_{40} = ca 10,000, where high permeability is achieved in directions parallel and perpendicular to the rolling direction. These latter generally are used in audio and instrument transformers, instrument relays, for rotor and stator laminations, and for magnetic shielding. Typical permeability–flux density curves for a 0.35-mm thick, transformer-grade lamination at various frequencies are given in Figure 5, and the magnetic properties of thin-gauge (0.1 mm) material suitable for cut-cores and tape-wound cores are illustrated in Figure 6. A three- to fourfold increase in initial and maximum permeability can be achieved by annealing alloys of ca 56–58 wt% Ni in the presence of a magnetic field after the usual high temperature anneal. The 56 wt% alloy listed in Table 4 is so treated.

For 79 wt% Ni, most modern alloys contain Mo (4–5 wt%) or Cu plus Mo (4 wt% Mo–4.5 wt% Cu–77 wt% Ni). Two grades are available: a standard grade, μ_{40} = ca 35,000, and a very high permeability grade, μ_{40} = ca 60,000. The latter is based on the development of Supermalloy (22) with $\mu_{40} > 100,000$ and where impurities, eg, C (ca 0.01 wt%) and Si (ca 0.15 wt%), are minimized and careful attention is paid to melting and fabrication practice. Practically all alloys of both grades are melted in vacuum. The general applications of the 79 wt% Ni alloys are the same as for the 50 wt% Ni alloys especially where superior qualities are sought and, in particular, where compactness and weight factors are important. Magnetic properties are compared with those of other alloys in Figures 2, 5, and 6.

Other developments include the attainment of high permeability at cryogenic temperatures (23) for shielding applications inside liquid nitrogen or helium chambers, and temperature stability of μ_i near room temperature (24) which is required in earth-leak transformers.

Square-Loop Alloys. Three classes of square-loop Ni–Fe alloys have been developed. In one class (50 wt% Ni), squareness is obtained through the development of cube texture, {100} ⟨001⟩, in the sheet. The texture results from extensive rolling (>95%) followed by primary recrystallization at ca 1100–1200°C. The use of cube texture to square the hysteresis loop also is possible in the 79 wt% Ni alloys, but the composition and heat treatment must be chosen such that $K_1 > 0$, ie, ⟨001⟩ is an easy axis of magnetization. The most recently developed class of square-loop alloys, which are centered around 65 wt% Ni, are characterized by a squareness that is like that of the 50 wt% Ni alloy and superior to that of the 79 wt% Ni alloys and by a saturation induction that is intermediate between the two. Representative hysteresis loops are illustrated in Figure 7; the magnetic properties are given in Table 4. The 3 wt% Mo–65 wt% Ni alloy (Mo is added for increased resistivity) is unoriented, and squareness is obtained by annealing in a magnetic field.

It also is possible to develop square hysteresis loops via the slip-induced anisotropy through plastic deformation. This technique had been employed in the commercial processing of Twistor memories (25) no longer used in telephone electronic systems.

Skewed-Loop Alloys. Skewed loops exhibiting Isoperm characteristics, ie, low remanence and constant permeability, are obtained by the development of a magnetic anisotropy where the easy axis is perpendicular to the direction

of an applied field. Isoperm, a 50 wt% Ni alloy, is obtained by rolling a cube-textured material; the source of anisotropy is slip-induced. Ultraperm F and Permax F are obtained by magnetic annealing in a transverse field. The advantages of magnetic annealing vs rolling are lower coercivity and higher permeability.

Other. Molybdenum Permalloy powder of ca 2 wt% Mo–81 wt% Ni is used to prepare cores for applications, eg, high *Q* (quality factor) filters, loading coils, resonant circuits, and radio frequency inductors (RFI) filters. Generally, a range of permeabilities from ca 15–550 is available commercially having operating frequencies as high as 300 kHz for the low permeability cores. As compared to ferrites, Permalloy cores have higher saturation and hence superior inductance stability after high d-c magnetization, but the Permalloy cores cannot compete at high frequencies because of their lower resistivity.

Nickel is being used in magnetostrictive transducers in some ultrasonic devices, eg, soldering irons and ultrasonic cleaners, because of its moderate magnetostriction and availability. This market, however, is dominated by piezoelectric transducers of lead zirconate–titanate (PZT) .

Ni alloys of 30–32 wt% are used as temperature-compensator alloys and are characterized by a steep decrease in magnetic permeability with temperature. These alloys are ideally suited in electrical circuits as shunts which maintain constant magnetic strength in devices such as electric meters, voltage regulators, and speedometers.

The thermal expansivity of Ni–Fe alloys vary from ca 0 at ca 36 wt% Ni (Invar [12683-18-0]) to ca $13 \times 10^{-6}/C^{\circ}$ for Ni. Hence, a number of compositions, which are available commercially, match the thermal expansivities of glasses and ceramics for sealing electron tubes, lamps, and bushings. In addition, the thermal expansion characteristic is utilized in temperature controls, thermostats, measuring instruments, and condensers.

3.5. Iron–Cobalt Alloys. Iron–cobalt alloys have the highest values of saturation induction at room temperature, at 2.45 T (2.45×10^4 G) for the 35% Co alloy. Commercial alloys of ca 35% Co, with 0.5% Cr added to improve ductility and to increase the resistivity, are known as Hipercos. A 27 wt% Co Hiperco is being produced as of this writing. Somewhat lower values of saturation induction but substantially higher permeability are obtained in equiatomic alloys because of low magnetocrystalline anisotropy. Commercially important equiatomic alloys are 2V Permendur [37188-80-0] and Supermendur which contain 49 wt% Fe, 49 wt% Co, and 2 wt% V. Iron–cobalt alloys are costly because of the high price of cobalt and because fabrication is difficult. These alloys are used for specialized applications, eg, aircraft generators, where the high saturation induction permits weight and size savings. These alloys also are used for receiver coils, switching and storage cores, high temperature components, as diaphragms in telephone receivers because of the high incremental permeability over a wide induction range, and to a limited extent as magnetostrictive transducers because of the large magnetostriction at ca 50 wt% Co.

The Fe–Co alloys exist in the fcc structure above 912–986°C to ca 70 wt% Co. Below this temperature range, the structure changes to bcc. At ca 50 wt% Co, the material further orders to the CsCl-type B2 structure below about 730°C and becomes very brittle. The addition of V in Permendur retards the

rate of ordering and imparts substantial ductility to the alloy, although quenching is necessary. Vanadium addition also increases the resistivity, eg, from 7–26 $\mu\Omega \cdot$ cm using a 2% addition.

Supermendur is prepared by using the highest purity commercial ingredients, by melting in a controlled atmosphere furnace and by using wet and dry hydrogen treatments so as to remove interstitial impurities, and by annealing in a magnetic field (26). The result is large maximum permeability and low coercivity. A comparison of the properties of various commercial Co–Fe alloys is given in Table 5 and in Figure 2.

Although 2V Permendur is sufficiently ductile to permit extensive rolling to thin gauge, controlled heat treatments are required for the development of superior strength and ductility combinations which permit application in high speed rotors (28,29). The addition of 4.5 wt% Ni to the 2V–49Co alloy results in enhanced ductility and strength over a wide heat-treating temperature range, thus eliminating the need for relatively close control (30).

3.6. Soft Ferrites. The name ferrite without qualifiers implies the spinel oxide having the general formula $MOFe_2O_3$. Commercially important ferrites contain two or more metallic elements M, and the iron content usually deviates from stoichiometry with consequent improvement in magnetic properties. Soft ferrites, ie, those having low coercivity, also include garnets typified by the formula $R_3Fe_5O_{12}$, where R is yttrium or a rare earth. The electrical resistivity of ferrites usually is 10^6 times that of metals. Ferrite components, therefore, have much lower eddy-current losses and, hence, are used at frequencies above about 10 kHz.

The magnetic properties of ferrites are intricately related to composition, microstructure, and processing much more so than in the case of metals primarily because of the complex chemistry of the oxides and because of the ceramic processing required to produce the finished parts.

Inductors and Transformers. For communication transformers involving low flux densities, the most important magnetic requirement is high initial permeability. Ferrites operating in this linear range of the B/H curve are linear ferrites. The most widely used linear ferrite is MnZn ferrite having values of μ_i, typically measured at 10 kHz and $H = 0.4$ A/m (5 mOe), up to 18,000 available commercially. A value of $\mu_i = 40,000$ has been achieved in the laboratory (31). The relevant properties of some typical materials are listed in Table 6. Generally, the higher the permeability, the lower the useful frequency range is before the permeability drops off significantly.

Optimum permeability is achieved by choosing the composition where the anisotropy constants K_1 and λ are near zero, by using high purity raw materials, and by controlling the sintering process to achieve highly dense material with uniform large grain sizes without significant loss of ZnO. The composition region where high μ ferrites have been produced (33) showing regions of low temperature coefficient (α/μ_i), low loss ($\tan \delta/\mu_i$), and low disaccommodation (D/μ_i) is illustrated in Figure 8. For transformers, eg, those used in switching power supplies for computers and other electronic products, a combination of high saturation induction, high permeability, and low loss is desired. Deflection yoke cores, flyback transformers, convergence coils, etc, for television receivers constitute the

largest usage of ferrites in terms of material weight. The property requirements, however, are far less severe than those for telecommunications components.

For inductors, the important magnetic requirements are low loss in combination with moderate permeability, small temperature coefficient of permeability, and small disaccommodation. MnZn ferrites generally are used to ca 1 MHz, beyond which NiZn ferrites having electrical resistivities about 10^4–10^5 times higher than MnZn ferrites are used. In MnZn ferrites, the bulk resistivity is increased through additions, eg, Ca and Si, which segregate to the grain boundaries, thereby providing insulating films. Through carefully controlled additions and by starting with homogeneous, high purity powders prepared by chemical coprecipitation techniques, ferrites have been developed with losses as low as 0.8×10^{-6} for tan δ/μ_i at 100 kHz (34). The use of MnZn ferrite cores in power transformers has increased rapidly as operating frequencies of power supplies rises. Power ferrites exhibit power losses at 200 kHz of less than 500 mW/g at 100°C. The loss tangent tan $\delta = \mu'/\mu'$ is the ratio of the imaginary component μ' of the complex permeability to the real component μ'. Losses as low as $0.3 \times 10^{-6} \tan\delta/\mu_i$ have been achieved using CO^{2+} additions to stabilize the domain walls (33). The low loss properties of both materials are easily degraded by magnetic and mechanical shock and, hence, are very difficult to achieve in manufactured components. The properties of some typical low loss commercial MnZn and NiZn ferrites are listed in Table 6. Domain-wall stabilization using CO^{2+} has also been successful in reducing loss in NiZn ferrites (35,36).

Disaccommodation denotes a change (generally a decrease) of permeability with time and is undesirable for filter inductors in terms of frequency instability. This phenomenon is attributed to the diffusion of Fe^{2+} ions; hence, both Fe^{2+} and vacancy contents are detrimental. In technical ferrites, a certain amount of Fe^{2+} is needed and, consequently, the disaccommodation is minimized by decreasing the vacancy content through controlled-atmosphere sintering and cooling and through the use of additives (37).

Microwave Ferrites. Microwave devices employing ferrites make use of the nonreciprocal propagation characteristics that are close to or at a gyromagnetic-resonance frequency at ca 1–100 GHz. The most important devices are isolators and circulators (see MICROWAVE TECHNOLOGY).

Properties that are important for microwave devices include saturation polarization J_s and its temperature dependence T_c, resonance line width ΔH, and dielectric constant. Materials having a range of J_s are needed, depending on the operating frequency φ of the device, since for resonance, $J_s < \omega/\lambda$ where λ is the gyromagnetic ratio. Thus, in the low frequency range of 1–5 GHz, garnets, eg, yttrium iron garnet (YIG), with various substitutions and having a range of $J_s = 0.02 - 0.18$ T (200–1800 G) are used. In the intermediate frequency range of 2–30 GHz, MgMn, MgMnZn, and MgMnAl ferrites with $J_s = 0.06 - 0.25$ T (600–2500 G) are used along with the garnets. At high frequencies in the millimeter wave region (30–100 GHz), NiZn ferrites having J_s up to 0.50 T (5000 G) are used. The garnets have particularly small linewidths. Single crystals have values of ΔH as low as 0.3 A/cm (0.4 Oe) as compared to ca 40 A/cm (50 Oe) for the MgMn ferrites. In polycrystalline material, grain boundaries and porosity also increase the linewidth. Hence, sintering to high density with large grain size is important, and values of $\Delta H = 0.6$ mA/cm

(0.75 mOe) have been reported (38). Examples of commercial microwave ferrites are listed in Table 7.

3.7. Amorphous Soft Magnetic Alloys. Although most alloys solidify to a crystalline structure, several transition-metal (Fe, Co, and Ni)$_{80}$-metalloid (B, C, Si)$_{20}$ alloys become amorphous when quenched from the liquid state at a sufficiently rapid rate. These can be quenched into the form of thin continuous ribbons and sheets and are commercially available as Metglass (AlliedSignal Corp.) for use in power distribution transformers (up to 500 W) which are being installed in the United States at the rate of one million per year. The amorphous alloys are atomically disordered and thus exhibit a lower density, higher resistivity (about a factor of three, $\sim 150\,\mu\Omega \cdot$ cm), small macroscopic anisotropy, and the absence of grain boundaries than their crystalline counterparts such as grain-oriented silicon transformer steels. This results in a lower eddy-current core loss (41,42) leading to an annual saving of power exceeding several hundred million dollars per year. The material price, since 1978, has dropped by a factor of 100. For low power electronic applications, several amorphous alloys are comparable to the Ni–Fe crystalline alloys. There are at least nine commercially available Metglass (amorphous) alloys (see GLASSY METALS).

The useful amorphous magnetic alloys can be conveniently grouped into the three classes given in Table 8. The iron-based alloys having saturation inductions in the 1.6–1.8 T range are substituted for grain-oriented silicon steels in power distribution applications, and with appropriate modifications in composition and heat treatment, possess good high (up to 100 kHz) frequency properties comparable to or better than those of crystalline nickel–iron alloys. The amorphous iron–nickel-based alloys exhibit lower magnetostriction and better corrosion resistance than the iron-based alloys, but are more expensive. The amorphous cobalt-based alloys exhibit nearly zero stress sensitivity and the highest permeabilities, but are the most expensive.

3.8. Uses of Soft Magnetic Materials. Because of low resistivity, iron and low carbon steels tend to be used in static applications, eg, pole pieces for electromagnets and cores for d-c magnets or relays. Low carbon steels and the lower grade Fe–Si alloys are used in small motors and generators. The higher grade Fe–Si alloys have traditionally been used in power distribution transformers and large rotating machinery, but certain amorphous iron–metalloid alloys are increasingly being used in the manufacture of distribution transformers by General Electric, Westinghouse, and Osaka, for example. Fe–Al and Fe–Al–Si alloys are used primarily as recording head materials because of their high hardness, resistivity, and saturation magnetization. Ni–Fe alloys used widely in high quality relays, transformers, converters, and inverters in the electronics industry, have much higher permeability and lower loss than Fe–Si alloys. The Co–Fe alloys are used because of their higher saturation polarization (flux density) and Curie temperature, but have the disadvantage of poorer workability and higher cost. Because of their exceptionally higher resistivities, ferrites are particularly suitable for high frequency applications.

4. Hard Magnetic Materials

Hard or permanent magnetic materials are characterized by high coercivity and high energy product. The important commercial hard magnetic materials as of 1994 are ferrites, rare-earth (R)-cobalt alloys, and the ternary alloys based on $Nd_2Fe_{14}B$. The last exhibit the highest coercivities and energy products. The use of Alnico and the binary R–Co alloys has continually decreased because of the high cost of cobalt. These are being replaced by the ternary NdFeB materials. The total market for permanent magnet materials in 1987 was estimated to be about 1.46×10^9 U.S. dollars: ferrites had 65% of the market, R–Co alloys 18%, NdFeB 4%, Alnicos 11%, and others 2%. Because of the superior magnetic properties and cost advantage, the market share of NdFeB magnets had increased to 16% by 1990.

Rare-earth magnets exhibit coercivities in excess of 600 kA/m (7.5 kOe) and energy products up to 290 kJ/m^3 (36×10^6 G · Oe). The newer Cr–Co–Fe alloys have magnetic properties similar to the Alnicos but have the advantage of being cold formable. Thus these alloys are classed with Cunife and Vicalloy in the family of ductile hard magnets. Physical and magnetic properties of selected hard magnetic materials are given in Tables 9 and 10 (44–48). The progress in energy products for hard magnetic materials is shown in Figure 9 and representative demagnetization curves of some of these materials are illustrated in Figure 10.

4.1. Alnicos. Alnico is a family of iron-based alloys containing Al, Ni, and Co plus about 3% Cu. A few percent of Ti and/or Nb is added in the higher coercivity alloys (Alnicos 6–9). Alnicos 1–4 are isotropic, whereas Alnicos 5 and up are anisotropic as a result of being heat-treated in a magnetic field. The anisotropic magnets are known as Alcomax and Hycomax in the U.K. and as Ticonal in Holland. Alnico 5 is the most widely used of the family. Because of their brittle nature, the Alnicos are produced by casting or by power metallurgy. The sintered alloys generally are mechanically stronger but magnetically weaker as a result of, among other factors, incomplete densification. They are used primarily in large quantity production of small articles of complex shape because surface grinding is the only possible finishing method for the Alnicos.

Above the solution treatment temperature (ca 1250°C), the alloy is single phase with a bcc crystal structure. During cooling to ca 750–850°C, the solid solution decomposes spinodally into two other bcc phases α and α' which differ little in lattice parameter composition. The matrix α-phase is rich in Ni and Al and weakly magnetic as compared with α', which is rich in Fe and Co. The α'-phase tends to be rod-like in the $\langle 100 \rangle$ direction and ca 10 nm in diameter and ca 100 nm long. As the temperature is decreased, segregation of the elements becomes more pronounced and the difference between the saturation polarizations of the two phases increases.

It generally is accepted that the mechanism of coercivity in the Alnicos is incoherent rotation of single-domain particles of the α'-phase based on shape anisotropy. As coercivity increases, the larger the aspect ratio of the rods and the smoother their surface becomes; the difference between the saturation polarizations of the two phases also increases. It is thought that Ti increases

the coercivity of Alnico because of an increased aspect ratio of the rods and a smoother surface.

If the decomposition reaction takes place below the Curie temperature, which is the case for anisotropic Alnicos, and if a magnetic field is applied during the decomposition, the α' rods tend to form along the $\langle 100 \rangle$ direction closest to the field direction so as to minimize the magnetostatic energy. This effect was first demonstrated in an Alnico 5 single crystal using electron microscopy (49). The result is an increase in H_c, B_r, and $(BH)_{max}$ in the field direction at the expense of the direction normal to it. This is the origin of improved magnetic properties in the anisotropic magnets shown in Table 10.

Some of the composition adjustments in the Alnicos result in a high Curie temperature so that the decomposition reaction can take place relatively rapidly below T_C. This is particularly true for Co, which is 24 wt% or greater for the anisotropic magnets. Another important consideration is the suppression of nonmagnetic fcc γ-phase which may appear at 1000–1100°C; in this regard, the amount of Al, which is a γ-suppressor, is critical. The formation of γ is pronounced if the Al content falls much below 7–8 wt%.

Isotropic Alnicos. Alnicos 1–4 in Table 10 are isotropic because the Curie temperatures are too low, as a result of the low Co content, for magnetic-field treatment to be effective. A typical heat treatment consists of solution treatment at 1250°C, controlled cooling to room temperature, and aging at ca 600°C with controlled slow cooling or step-aging at successively lower temperatures. The maximum energy is ca 12 kJ/m^3 (1.5×10^6 G · Oe).

Anisotropic Alnicos. Alloys composed of about 24% Co, ie, Alnicos 5 and 6, develop anisotropic properties by heat treatment in a magnetic field, generally ca 80 kA/m (1.0 kOe). This is accomplished by cooling from the solution treatment temperature at an average speed of about 1C°/s, by taking the magnets out of the solution treatment furnace and putting them in the field of an electromagnet, solenoid, or permanent magnet. The field needs to be only from 750–850°C while the spinodal decomposition occurs. The primary difference between Alnicos 6 and 5 is a 1% Ti addition in Alnico 6 which results in an increase in H_c at the expense of B_r and energy product.

High H_c Alnicos. The coercivities for Alnicos 8 and 8 HC of 120–160 kA/m (1.5–2.0 kOe) (vs ca 50 kA/m (0.6 kOe) for Alnico 5) are achieved by increasing the Co content to $\geq$35% and the Ti content to 5–8%. The coercivity of Alnico 8 HC is higher than that of Alnico 8 by virtue of the higher Ti content. Some of the Ti may be replaced by Nb; this is particularly true of alloys produced in the U.K. In contrast to Alnicos 5 and 6, the magnetic-field heat treatment of Alnicos 8 and 8 HC is conducted isothermally at ca 800°C instead of by continuous cooling. The isothermal heat-treatment temperature is critical ($\pm 2 - 3$°C) and is optimized for a given alloy.

Columnar Alnicos. Because the α' rods precipitate along $\langle 100 \rangle$ axes, the directional magnetic properties can be enhanced if the cast structure possesses a preferred $\langle 100 \rangle$ orientation among the grains. For the Alnicos, as for most materials with a cubic crystal structure, $\langle 100 \rangle$ is the preferred growth direction in the direction of heat flow during solidification. Hence, $\langle 100 \rangle$ textured material with columnar grain structure is obtained commercially by the use of heated molds and chill plates to achieve unidirectional heat flow. The result is a

squaring of the hysteresis loop with concomitant improvements in B_r, H_c, and $(BH)_{max}$. Values of $(BH)_{max} = 64$ kJ/m^3 (8×10^6 G · Oe) are offered commercially for Alnico 5 Col. A less effective but less expensive technique for achieving partial orientation is by the use of chill plates without heated molds. These are designated Alnico 5 DG in Table 10.

It is very difficult to achieve columnar structure in the Ti-bearing, high H_c alloys. Raw materials should be of high purity (50) and the addition of 0.2% S helps promote columnar grain growth (51). The latter technique is most likely used in the commercial production of Alnico 9, which is the columnar version of Alnico 8 and contains 5% Ti. Columnar grain growth for the 8% Ti alloy is more difficult because of grain nucleation from oxides, nitrides, and carbides in the melt. The Magnicol process (52) has been successful for commercial production (44). The technique involves deoxidation of the melt using Si and C followed by the addition of sulfur. The properties of two grades (Col. Alnico HC) having peak values for $(BH)_{max}$ ca 92 kJ/m^3 (11.6×10^6 G · Oe) and H_{cB} ca 175 kA/m (2.2 kOe) (53) are listed in Table 10.

4.2. Hard Ferrites. Hard ferrites, general formula $MO6Fe_2O_3$, where M is Ba or Sr, are hexagonal in crystal structure. Most commercial ferrites are barium ferrites. These have dominated the market since their introduction in 1952. More recently, strontium ferrite is being produced in large quantities as it has superior properties compared with barium ferrite. Ferrites are produced by ceramic techniques and the magnets are often called ceramic magnets (Table 10). Ferrite powders are often bonded in plastic or rubber for low cost, large volume production, especially when complex shapes are required. These are known as bonded magnets and because they are flexible, they find wide use. The 3M Co. manufactures flexible magnet strip under the name Plastiform.

The origin of large coercivity in the hard ferrites lies in the large magnetocrystalline anisotropy ($K_1 =$ ca 0.3 MJ/m^3 (3×10^6 erg/cm^3)) combined with low saturation polarization ($J_s =$ ca 0.47 T (4700 G)). Strontium ferrite has a somewhat larger K_1 and smaller J_s as compared with barium ferrite. Because the Curie temperature is rather low (ca 450°C), the magnetic properties are much more temperature sensitive than for the Alnicos. Remanent induction decreases with increasing temperature at a rate of $0.19\%/C^\circ$ and the intrinsic coercivity decreases with decreasing temperature at a rate of $0.2 - 0.5\%/C^\circ$. Exposure to low temperatures can lead to serious demagnetization problems as a result of reduced H_{cJ}. Thus some of the commercial hard ferrites were developed to have high H_{cJ} values, eg, Ceramics 4 and 7 in Table 10.

A typical ferrite magnet is prepared by first mixing iron oxide and $BaCO_3$ or $SrCO_3$. The mixed powder is calcined at ca 1100–1200°C to form the ferrite. The aggregate is ball-milled to ca 1 μm, pressed in a die, and sintered to high density at ca 1200°C. In general, the grain size is finer and a lower sintering temperature is used resulting in a higher coercivity and lower remanence. Anisotropic magnets are prepared by aligning the powder in a magnetic field during the pressing operation. The exact composition of typical commercial ferrites (Table 10) usually is not given. Lead may be present in a small amount in Sr or Ba ferrite to facilitate sintering.

One of the fastest-growing areas in hard magnetic materials is the plastic-bonded ferrite where the milled calcined ferrite powder is embedded in a plastic

(see EMBEDDING). Both isotropic and anisotropic grades are prepared. Although the magnetic properties are inferior (see Table 10), the plastic-bonded magnets are inexpensive, can be cut and drilled, and can be made flexible. Large quantities are used in door catches, wall magnets, refrigerator-door gaskets, board games, toys, and small motors.

Because one advantage of ferrites over the other hard magnetic materials is low price, innovations in the industry tend toward lowering production costs. Much attention has centered on the substitution of low cost, impure raw materials for the more expensive high quality ones. Celestite may be used as a cheap source of Sr (54); it is primarily $SrSO_4$ and contains varying small amounts of $CaSO_4$, $BaSO_4$, SiO_2, and Al_2O_3. Natural hematite is much cheaper than synthetic oxide, but contains small amounts of SiO_2 and Al_2O_3. Not only do the impurities affect the calcining and sintering behavior of the ferrite, but the size, shape, size distribution, and the chemical perfection of the starting materials also have a profound and complicated effect. Unlike other hard magnetic materials that contain Co and/or rare earths, the raw materials for the ferrites generally are inexpensive, plentiful, and nonstrategic. Thus the conversion of Alnico to ferrite in loudspeakers and d-c motors has accelerated.

Uses. Hard ferrites are used widely in electromechanical devices, eg, generators, relays, motors, and magnetos; electronic applications, eg, loudspeakers, traveling-wave tubes, and telephone ringers and receivers; antitheft tags, holding devices such as door closers, seals, and latches; and are perennial favorites in various toy designs. Loudspeakers are the largest use of permanent magnets (ca 50%). Strontum ferrites exhibit higher coercivities and are increasingly being produced.

4.3. Cobalt–Rare-Earth Magnets. The origin of magnetism in the rare-earth (R) transition-metal intermetallic compounds is the interatomic exchange between the spins of the two sublattices plus the spin-orbit coupling between the rare-earth atoms. The magnetocrystalline anisotropy also comes from two sources, one originating in the itinerant electrons of the Co sublattice in the R–Co phases and one caused by the crystalline electric field of the rare earths. Reviews of magnetism in the rare-earth transition-metal compounds are given in References (55–61). Of the large number of rare-earth transition-metal compounds only a few, ie, RCo_5, $R_2Co_{17}(RCo_{8.5})$, particularly the Sm series outside of the newest rare-earth ternary intermetallics based on $Nd_2Fe_{14}B$, are the most prominent high performance hard magnets.

As shown in Table 11, several of the cobalt–rare-earth alloys exhibit moderate values of saturation polarization J_s (ca 1 T (1×10^4 G)) and extremely high values of magnetocrystalline anisotropy ($K_1 > 1$ MJ/m^3 (10^7 erg/cm^3)). The latter is primarily responsible for the large coercivity. The R_2Co_{17} compounds have a hexagonal crystal structure with either the Th_2Ni_{17} (hexagonal) or the Th_2Zn_{17} (rhombohedral) modification. Both have RCo_5 as subcells and differ only in stacking sequence. These compounds generally exhibit a higher value of J_s than the corresponding RCo_5 series and result in a greater energy product. However, with the exception of Sm, Er, and Tm, all the 2–17 binary compounds have $K_1 < 0$, ie, an easy (0001) plane. Low coercivity is expected for the $K_1 < 0$ compounds.

The first rare-earth magnets, developed in the 1960s and commercially produced in the 1970s, were based on the intermetallic compounds RCo_5 and R_2Co_{17}.

$SmCo_5$ has the hexagonal $CaCu_5$ structure, a moderate saturation induction (Table 11), and extremely high positive values of magnetocrystalline anisotropy. Magnets based on $SmCo_5$ are single phase. Laboratory magnets have attained values $B_r = 1\text{T}(1 \times 10^4\ \text{G})$ $H_{cJ} = 3200$ kA/m (40.2 kOe) and $(BH)_{\max} = 200\ \text{kJ/m}^3$ $(25\text{MG} \cdot \text{Oe})$. Commercial magnets are characterized by $(BH)_{\max}$ from $130 - 160\ \text{kJ/m}^3$ $(16 - 20\text{MG} \cdot \text{Oe})$. The coercivity of these magnets is based on nucleation of domains and wall pinning at grain boundaries. Plastic-bonded magnets are also in production.

Sm_2Co_{17}, also hexagonal, has a higher saturation induction but a lower value of K_1. Commercial magnets based on $SmCo_{8.5}$ contain, in addition to Co, the metals Cu, Fe, and Zr substituted for some of the Co. The good hard magnetic properties arise from microstructural precipitates which inhibit (pin) domain walls. A commercial alloy of $Sm(Co_{0.68}Cu_{0.10}Fe_{0.21}Zr_{0.01})_{7.4}$ exhibits values of $B_r = 1.10\text{T}$ $(1.10 \times 10^4\ \text{G})$, $H_{cJ} = 520$ kA/m (6.5 kOe) and $(BH)_{\max} = 240\ \text{kJ/m}^3$ $(30\ \text{MG} \cdot \text{Oe})$. Values of $(BH)_{\max} = 264$ kJ/m $(33.2\ \text{MG} \cdot \text{Oe})$ have been achieved in the laboratory. Representative magnetic properties and typical demagnetization curves are given in Tables 9, 10 and 11 and Figure 10, respectively.

The mechanism of coercivity in single-phase $SmCo_5$ magnets is based on nucleation and/or pinning of domain walls at surfaces or grain boundaries. Large values of coercivity can be achieved only in fine particle form (1–10 μm) or in fine-grained sintered magnets prepared from such powders. Thus fabrication techniques are based on powder metallurgical procedures, including alignment in a magnetic field during the pressing operation.

Other RCo_5 single-phase hard magnets in addition to Sm have been prepared both commercially and in the laboratory. These include Sm in combination with Pr, Ce, and Ce-mischmetal (CeMM), this last a very low cost mixture containing about 55% Ce, 25% La, 13% Nd, and 5% Pr. (Pr,Sm)Co_5 magnets have higher values of saturation induction than $SmCo_5$, but are produced only in a limited way. The Sm–Ce and Sm–CeMM combinations lower the magnetic properties, but the price of raw materials is lower.

Partial substitution of Co by Cu in $SmCo_5$ and $CeCo_5$ results in fine-scale (ca 10 nm) precipitation at low temperatures (400–500°C) (55,60). The precipitate is a phase that is coherent with the RCo_5 structure that develops into R_2Co_{17} particles upon coarsening beyond the maximum coercive force point. Unlike the single-phase magnets, the coercivity mechanism here is based on homogeneous pinning of domain walls at the precipitate particle; thus magnetic hardening is possible with bulk material, and high energy product magnets can be produced in directionally solidified samples similar to the columnar Alnicos. However, commercial practice also is based on powder metallurgy because magnets that are prepared by powder metallurgical techniques have better mechanical properties and improved magnetic alignment.

The large values of maximum energy product and coercivity of the rare-earth magnets permit use in devices where small size and superior performance are desired (62). Magnets for electronic wristwatches and for traveling-wave tubes are largely made of rare-earth alloys. There are medical device applications which make use of the RCo_5 and R_2Co_{17}-base alloys. The temperature coefficient of polarization, which is typically $-0.04\%/°\text{C}$, is too high for precision

applications, such as gyros and accelerometers. However, polarization of the heavy RCo_5 compounds, eg, Co_5Dy, increases with temperature at ca 25°C. When these rare earths are mixed with Sm, the temperature coefficient can be reduced by partially replacing the Sm with a heavier rare earth such as Dy.

4.4. $Nd_2Fe_{14}B$ Family of Magnets and Related Materials. The high cost of cobalt and samarium stimulated investigation and development in the early 1980s of low cost permanent magnets to replace the Co–Sm-based materials. Ternary metal alloy systems containing Fe and the cheaper rare-earth metals Ce, Nd, and Pr were investigated. This led to the discovery of the ternary intermetallic boride $Nd_2Fe_{14}B$ (63,64). Developed in 1983 by Sumitomo special metals and General Motors (65,66), magnets based on the ternary $Nd_2Fe_{14}A$, where A = B C, N, exhibit the highest magnetic performance (Table 8 and Figs. 9 and 10). These materials are largely replacing the commercial R–Co ones.

The theoretical maximum energy product for $Nd_2Fe_{14}B$ is approximately 64 MG · Oe (512 kJ/m^3) (67), 2.5 times greater than for $SmCo_5$. Energy products for the commercially available magnets (200 – 300 kJ/m^3) are less than theoretical but well in excess of the 130 – 160 kJ/m^3 exhibited by $SmCo_5$. $Nd_2Fe_{14}B$, like $SmCo_5$, is brittle and several manufacturing techniques have been developed for forming this material into usable shapes. As of this writing, permanent magnets based on this material are the best available.

The crystal structure of $Nd_2Fe_{14}B$ is tetragonal, the unit cell contains four formula units, and the space group is $P4_2mmm$ (68,69). There are crystal structure features similar to the hexagonal RCo_5 phases. The Nd–Fe atomic moments are coupled parallel, ie, ferromagnetically, similar to the Co-light R phases, but antiparallel to the heavy R-atoms leading to lower net magnetizations (ferrimagnetic). Thus the net magnetization of $Nd_2Fe_{14}B$ is approximately 1.6 T (16,000 G).

The energy product $(BH)_{max}$ is a measure of a magnet's resistance to demagnetization in reverse fields, thus a high coercivity along with the saturation magnetization is required for a large energy product. The easy axis of magnetization in $Nd_2Fe_{14}B$ is the crystallographic *c*-axis and it is the origin of the high coercivity exhibited by this material. To rotate the magnetization from the *c*-axis to an axis normal to it (*a*-axis) or hard axis, a high applied field must be used. The field required to do this is called the anisotropy field, H_a. This is the upper limit of the coercivity; the practical coercivity is sensitive to details of the microstructure, ie, effected by impurity phases and grain boundaries, and seldom exceeds 10–20% of the anisotropy field. The contribution of the Nd and Fe ions to H_a (65) are sufficiently high for development of high energy product magnets. The isostructural $Pr_2Fe_{14}B$ phase is the only one of the other ternary boride materials that exhibits high magnetization and H_a for development of practical hard magnetic materials.

The Curie temperature for $Nd_2Fe_{14}B$ ($T_C = 312$°C), as well as those for all of the other $R_2Fe_{14}B$ type-phases, are lower than those for the RCo_5 and R_2Co_{17} phases but higher than the R_2Fe_{17} phases (Table 12) (66). For many applications, high values of T_c are desirable, because this leads to a smaller temperature dependence of magnetic properties and higher temperature applications. Substitution of small amounts of Dy and Co for a part of the Nd and Fe, respectively,

improves Curie temperature and temperature dependence but at the expense of lower magnetization and higher material price.

Research has been directed toward discovery of lower cost ternary permanent magnet materials having even better properties, ie, higher saturation coercive force and Curie temperatures, than $Nd_2Fe_{14}B$. A summary is shown in Table 12. $Nd_2Fe_{14}C$ exhibits a lower Curie temperature and smaller values of intrinsic magnetic properties and suffers from difficulties in preparing suitable castings by normal procedures prior to grinding. A promising nitride is $Sm_2Fe_{17}N_{2.7}$. As of this writing (ca 1994) development is under way for commercialization of this material (70,71) (see NITRIDES). A summary of developments of other materials appears in Reference 72.

Sintered Magnets. $Nd_2Fe_{14}B$ is brittle, similar to the ferrites and RCo_5 materials, and the manufacture of useful shapes can be made by a conventional powder forming process. In general, melting and casting of the material are done in an inert atmosphere, usually argon, and the castings are crushed and milled to powder below 10 microns in size, then aligned in a magnetic field, pressed into desired shapes and sintered at about 1100°C and cooled rapidly. An enhancement in coercivity can be obtained by a post-sintering heat treatment. The particle alignment in a magnetic field results in a product referred to as anisotropic magnets. If liquid-phase sintering is done to enhance density and coercivity, the starting composition is richer in Nd and B and the final microstructure will have a layer of Nd-rich and Fe–B-rich second phases at the grain boundaries. The Nd-rich second phase appears to enhance coercivity.

Melt Spun Magnets. Melt spun magnets refer to those manufactured from rapidly quenched melts of $Nd_2Fe_{14}B$. The quenched material is in the form of ribbon, 15–50-μm thick and approximately 1.5-μm wide, because the molten alloy liquid stream is directed at a rotating cold cylinder in an inert atmosphere so as to prevent oxidation. Depending on the rate of cooling, the microstructure can be amorphous, finely crystalline, or coarsely crystalline. Amorphous ribbon (over quenched) exhibits weak intrinsic coercivity, thus the grain or crystallite size can be finer than that obtained by the above conventional process. The optimally quenched ribbon is then crushed to powder which is then blended with a polymer, such as epoxy, and pressed at 600–700 MPa (87,000–100,000 psi) into bonded magnets by various molding techniques. The volume fraction of the powder is approximately 80% and such magnets are isotropic, ie, the crystallite's easy axis of magnetization (hexagonal *c*-axis) are randomly oriented, similar to the grains in the ribbon, and the magnets are referred to as being isotropic. Such magnets exhibit remanent magnetizations in zero applied field of 0.7T (ca 7.0 kG) and $(BH)_{max}$ of ca 70 kJ/m^3.

Hot pressing of melt spun powder at ca 100 MPa (14,500psi) and ca 670°C leads to nearly 100% dense magnets. Because some grain growth can occur during hot pressing, amorphous or overquenched powder is used as starting material to obtain the optimum grain size. Little grain texture results from this operation; only about 10% crystallographic alignment occurs and the magnets are essentially isotropic. Hot pressed isotropic magnets have been produced with energy products in the $80 - 160\ kJ/m^3$ ($10 - 20\ MG \cdot Oe$) range.

Hot pressing to produce substantial texture and magnetic anisotropy via plastic deformation is accomplished by a process referred to as die-upsetting

(73–75). Initial hot pressed isotropic samples are placed in a larger die cavity and pressed at temperatures about 700°C. Substantial *c*-axis alignment along the compression direction occurs. The microstructure consists of individual plate-like grains lying normal to the compression axis. By this process, the remanence is increased to 0.8–1.2 T and maximum energy products to over 250 kJ/m^3 (31 $MG \cdot Oe$). The effect of Nd content on induced anisotropy in hot deformed Fe–Nd–B magnets has been studied and shown that crystallographic alignment is only possible for magnets containing 12% Nd (76); a liquid phase is present at the grain boundaries during deformation. The die-upsetting route can be used to produce anisotropic bonded magnets. Die-upset magnets are reground to produce magnetically aligned powder subsequently encapsulated into plastic (74,77).

4.5. Uses. The commercial development of magnets based on this boride proceeded rapidly, and they are now being used in many diverse applications, for example, servo devices for machine tools, for over 30 d-c motors for fully equipped automobiles (windshield wipers, cooling fans, window and antenna lift motors, etc), magnetic resonance imaging (mri), computer disk drives, and medical device applications. Their largest use is in positioning motors for hard disk drives. New designs of electrical machines are taking place (78).

4.6. Chromium–Cobalt–Iron Alloys. In 1971, a family of ductile Cr–Co–Fe permanent-magnet alloys was developed (79). The Cr–Co–Fe alloys are analogous to the Alnicos in metallurgical structure and in permanent magnetic properties, but are cold formable at room temperature. Equivalent magnetic properties also can be attained with substantially less Co, thereby offering savings in materials cost.

Typical property values for Cr–Co–Fe magnets are $B_r = 1.0 - 1.3$ T ((1.0–1.3 G) $\times 10^4$, $H_c = 150 - 600$ A/cm (190–753 Oe), and $(BH)_{max} = 10 - 45$ kJ/m^3 ($1.3 - 5.7 \times 10^6 G \cdot Oe$). Some representative properties of commercially available materials and laboratory specimens are listed in Table 10. Very favorable permanent magnetic properties, equivalent to those of Alnico 5, were obtained in low cobalt (ca 10%) ternary alloys. As in the Alnicos, isotropic and anisotropic grades are available. The latter exhibits superior properties achieved by annealing in a magnetic field and/or uniaxial deformation between annealing and aging; uniaxial deformation is not possible with the Alnicos.

Developments up to 1978 are summarized in References 80 and 81. Metallurgically, the Cr–Co–Fe alloys possess the bcc (α) structure at elevated temperature (>1200°C). From ca 700–1200°C, the α-phase tends to coexist with the nonmagnetic γ-phase, ie, fcc. At higher Cr content, a brittle σ-phase also appears in this temperature range. The high temperature α-phase can be retained by quenching, in which case it can undergo spinodal decomposition to an Fe-rich α_1-phase and a Cr-rich α_2-phase with particles of ca 30 nm. This occurs at about 650°C, a temperature which falls off with decreasing Co content to ca 550°C for the Fe–Cr binary. Additions, eg, Zr, Nb, Al, V, and Ti, tend to enlarge the α-phase field at the expense of γ.

The mechanism for coercivity in the Cr–Co–Fe alloys appears to be pinning of domain walls. The magnetic domains extend through particles of both phases. The evidence from transmission electron microscopy studies and

measurement of J_s, H_c, and anisotropy vs T is that the walls are trapped locally by fluctuations in saturation magnetization.

Particle shape is very important as evidenced by the elongation and alignment of particles resulting from magnetic annealing and/or uniaxial deformation and the consequent improvement of the magnetic properties, primarily B_r and squareness. Ternary alloys containing ca 12% Co and 33% Cr have achieved values of $B_r = 1.2$ T (1.2×10^4 G), $H_c = 60$ kA/m (750 Oe), and $(BH)_{max} = 42$ kJ/m^3 (5.3×10^6 G · Oe) through deformation aging, whereby the alloy is first aged and then uniaxially deformed by drawing, followed by final aging (82). Such treatment also produced the highest energy product in the Cr–Co–Fe system to date, at 78 kJ/m^3 (9.8×10^6 G · Oe) for a 23Co–2Cu–33Cr alloy (83). The record for magnetic annealing treatment is 76 kJ/m^3 (9.5×10^6 G · Oe), for a 15Co–3Mo–24Cr alloy with ⟨100⟩ columnar grain structure. Good permanent magnet properties could be developed even in the 2–5% Co range, with values of $(BH)_{max} = 42$ kJ/m^3 (5.3×10^6 G · Oe) for a 5Co–30Cr alloy (84). These low Co alloys exhibit the highest ratio of $(BH)_{max}$ to Co content of all Co-based alloys. Thus Alnico 5 properties are achieved in Cr–Co–Fe alloys with a Co content less than half of that in Alnico 5, with added ductility. The very low Co alloys, however, require extremely long heat-treatment times because of the decreased kinetics of the spinodal decomposition. Deformation aged 23%Cr–23%Co–2%Cu exhibits $(BH)_{max}$ of 78 kJ/m^3 (9.75MG · Oe) (85).

It seems likely that the Cr–Co–Fe alloys could replace the ductile Cunife and Vicalloys and some of the Alnicos. A member of the Cr–Co–Fe alloy family called Chromindur (12Co–20Mo–68Fe) is used as the bias-magnet material for a telephone receiver. The Co composition was reduced from 15 wt% (46) to 10.5% (85,86). The magnet must be formed into cup shape. The cold ductility of the Cr–Co–Fe alloy permits high speed room-temperature forming which is economically advantageous over the slow hot-forming (1250°C) operation required for Remalloy.

4.7. Copper–Nickel–Iron and Copper–Nickel–Cobalt Alloys. Cu–Ni–Fe permanent magnet alloys are ductile. They can be stamped even in the hard magnet state, ie, after aging. The nominal composition for a commercial alloy, Cunife, is 60 wt% Cu, 20 wt% Ni, 20 wt% Fe. The hard-magnet state is developed by quenching from 1040°C, tempering at 650°C, cold drawing or rolling, and aging at 650°C. Anisotropic properties are developed by extensive deformation, with $(BH)_{max}$ values up to 12 kJ/m^3 (1.5×10^6 G · Oe). Typical commercial values are given in Table 10.

Because of their cold ductility, Cunife magnets are used in speedometer and timing motors where parts are precision stamped at high speed. However, the ingot cannot be hot worked and ingot sizes are limited by segregation to ca 3 cm in diameter. Cunico, similar to Cunife, has composition 29 wt% Co, 21 wt% Ni, and 50 wt% Cu. However, it is no longer produced commercially.

4.8. Vanadium–Cobalt–Iron Alloys. V–Co–Fe permanent-magnet alloys also are ductile. A common commercial alloy, Vicalloy I, has a nominal composition: 10 wt% V, 52 wt% Co, and 38 wt% Fe (Table 10). Hard magnetic properties are developed by quenching from 1200°C for conversion to bcc α-phase followed by aging at 600°C (precipitation of fcc γ-phase). The resulting properties are isotropic, with $(BH)_{max}$ ca kJ/m^3 (0.75 MG · Oe). Because it can be rolled to

very thin sheets, Vicalloy is used widely in antitheft labels in department store articles and library books.

The V–Co–Fe family with ca 50 wt% Co is rather versatile. The 2 wt% V alloy, 2V-Permendur and Supermendur, is a soft magnet, and alloys containing 3–5 wt% V (Remendur) develop semihard properties, ie, H_c = ca 14 – 50 A/cm (18–63 Oe). Some of the V may be replaced by Cr, as is done commercially in Germany.

4.9. Platinum–Cobalt. Until the advent of the rare-earth magnets, platinum–cobalt magnets represented the best combination of coercivity and energy product (H_{cJ} = 400 kA/m (5 kOe)) and $(BH)_{max}$ = 72 kJ/m^3 (9MG · Oe)). Optimum properties are achieved near the equiatomic composition, ie, ca 77 wt% Pt. The alloy is ductile, with the hard magnetic properties developed by controlled cooling from 1000°C followed by aging at ca 600°C. The principal applications have been in hearing aids, watches, and traveling-wave tubes. The rare-earth magnets have replaced, for the most part, PtCo in the latter applications because of the expense of platinum.

4.10. Molybdenum–Cobalt–Iron Alloys. Commercial magnets in the Mo–Co–Fe family often are called Remalloy or Comol or Comalloy. There are two important compositions: 17Mo–12Co–71Fe and 20Mo–12Co–68Fe. Magnetic hardening is developed through precipitation aging by oil quenching from 1250°C, followed by aging at 675°C. Values of $(BH)_{max}$ are about 10 kJ/m^3 (1.3×10^6 G · Oe) (Table 10).

The 20 wt% Mo Remalloy was used primarily in a single product, as the bias magnet in an armature-type telephone receiver which was produced in more than 10^7 units annually. Because hot forging is necessary in its manufacture, Remalloy receiver magnets have been replaced by the cold-formable Cr–Co–Fe magnets.

4.11. Magnet Steels. Magnet steels are carbon steels containing ca 1% C and various percentages of Co, W, and Cr. They are among the first steels made specifically for permanent magnets. The hard magnetic properties are developed by a quench from ca 1000°C to develop a martensitic structure. Hence, they also are known as martensitic steels. Properties of some representative magnet steels are listed in Table 10. These are used in considerable amounts for applications such as hysteresis motors.

4.12. Manganese–Aluminum–Carbon Alloys. Anisotropic Mn–Al–C permanent magnet alloys have been developed using warm working (87). Properties as high as B_r = 0.61 T (6100 G), H_{cB} = 220 kA/m (2.8 kOe) and $(BH)_{max}$ = 56 kJ/m^3 (7×10^6 G · Oe) have been obtained. A typical alloy composition is 70Mn–29.5Al–0.5C. After casting, a cylindrical ingot is solution-treated at 1100°C, quenched to 500°C, tempered at 600°C, and extruded at 700°C. Additional improvements were obtained by aging at 700°C following the extrusion. Typical values of magnetic properties are given in Table 10.

The Mn–Al–C magnets have good mechanical properties and can be machined readily. Their use could expand because manufacture does not require expensive raw materials. However, manufacture is restricted to warm extrusion, a relatively expensive process. Production, as of this writing, is limited to a single plant in Japan for internal consumption.

4.13. Semihard Alloys. Coercivities of semihard magnets are from 10 – 100 A/cm (12–126 Oe). A good number of them are used in hysteresis motors. The magnet steels Cunife and Vicalloy are commonly used. More recent development involves the use of semihard magnets in self-latching remanent-reed electrical contacts in the telecommunications industry (88). These consist of a pair of paddles of semihard magnetic material sealed in a glass tube. The contact between the pair can be opened or closed by current passing through an external coil which surrounds the contacts. The reed material must be sufficiently ductile to be drawn into wire of ca 0.50 mm in diameter, followed by flattening to ca a 0.2-mm thick paddle. Magnetic requirements call for high remanent induction ($B_r > 1.2$ T (12,000 G)) and controlled H_c (ca 25 A/cm (31 Oe)). Physical requirements call for good solderability and plateability (with noble-metal contact material), sealability (with glass of appropriate wetting behavior and thermal expansivity), and, preferably, low magnetostriction. The alloys listed in Table 13 can be classified into equiatomic Co–Fe alloys, Co-based alloys, and Fe-based alloys. Of these, Remendur and Nibcolloy are perhaps the most widely used.

Thermal expansion coefficient at 20–400°C $\times 10^6$, C – 1	Formability[d]	Plateability[d]	Solderability[d]	Sealability[d]
10.2	G	G	G	G
9.8	G			
11	G	G	P	G
12.1	G	G	G	G
ca 12	G			
ca 12	G			
12.5	G			
ca 12	G			
5	G	G	G	G
12.5	G	G	P	
13	G	G	G	
11.5	G	G	G	

5. Experimental Methods

5.1. Field Production. Although magnetic fields from the gap of a permanent magnet often are used for fast qualitative indication of magnetic effects, controlled fields in laboratory instrumentation usually are provided by a solenoid or an electromagnet. Most solenoids are made with insulated copper wire which is wound around a tube; an axial field is generated with the passage of current. Because of resistance (I^2R) heating, field strengths from practical solenoids are limited to ca 80 kA/m (1.0 kOe). The Bitter magnet is used to produce very high fields. The winding is composed of thin perforated disks of copper, and water under high pressure is forced through the holes for cooling. A field of ca 10 MA/m (126 kOe) can be produced and fields twice that have been reached.

Such installations, however, require an enormous amount of power and expense. Since the discovery in 1961 of high field Nb_3Sn superconductors, high fields up to ca 10 MA/m (126 kOe) are obtained routinely using superconducting solenoids that are compact and far less expensive. For fields up to ca 2 MA/m (25 kOe), electromagnets are very popular. An electromagnet consists of a pair of cylindrical iron cores, called pole pieces, around which is wrapped a coil of wire carrying a direct current which magnetizes the cores to saturation. The maximum field achieved in the air gap between the pole pieces, except for a small contribution from the coil, is J_s/μ_o or 1.7 MA/m (21 kOe) for iron pole pieces. Higher fields can be obtained by using tapered pole caps to concentrate the magnetic flux.

5.2. Field-Strength Measurement. The two most used methods of measuring magnetic fields are the ballistic method and the Hall-effect method. In the ballistic method, a search coil connected to a ballistic galvanometer or a fluxmeter is moved from the region of the field to a region outside the field. The induced emf produces a current through the galvanometer and causes a deflection which is proportional to the field strength. In the Hall-effect method, a small plate-shaped semiconductor sensing element that is connected to a current source develops an emf across the plate at right angles to the current i when placed in a field H normal to the plate. The magnitude of this Hall emf is equal to R_HiH/tV, where t is the thickness of the plate in meters and R_H is the Hall constant, eg, ca $10^{-9}\ \Omega \cdot m^2/A$ in a semiconductor, eg, InSb.

5.3. Magnetization Measurement. For weakly magnetic specimens, the magnetic susceptibility usually is measured in a magnetic balance. Most modern systems make use of commercial automatic analytical balances, with the sample in a magnetic field. By way of cooling and heating, the susceptibility can be measured over wide temperature ranges.

A Foner vibrating sample magnetometer is a technique for the measurement of magnetization of samples that range from weakly magnetic to strongly magnetic. In this technique, current passing through a loudspeaker-type device forces the specimen to vibrate vertically. The a-c signal induced by the specimen in a pair of detection coils is amplified and compared with that induced by a known magnet. The output signal is proportional to the magnetic moment of the specimen.

For the measurement of magnetization in hysteresis-loop measurements, a search coil consisting of several-turn windings around a specimen is connected to a fluxmeter whose output can be recoded on the y-axis of an x,y plotter. The x-axis records the field strength of the primary coil around the specimen. The whole procedure can be done conveniently in a hysteresigraph, whereby the induction is recorded automatically as the field is varied continuously.

6. Economic Aspects

The value of the U.S. magnetics market in 1980 exceeded $\$2 \times 10^9$. The annual world magnetic materials market in 1988 was $> \$5 \times 10^9$. The value of the components made from these materials is perhaps 20 or more times greater than $5 billion.

The manufacturers of permanent magnets include Hitachi which produces Alnico Grades 5–9 (Table 10) in cast form in various shapes of Grades 2 and 5 in sintered form as well as the rare-earth–cobalt (Hicorex); IG Technologies Inc., which produces Alnico, cast grades (Hyflux) 5,8,9 in various shapes, sintered, grades 2,5,8, cunife magnets, ceramic magnets (Indox) grades 1 and 5, and the rare-earth–cobalt Incor; Crucible Magnetics, which produces Alnico, cast grades 5,7, and 8, ceramic magnets (Ferrimag), and the rare-earth–cobalt Crucore; Arnold Engineering, which produces Alnico, cast grades 5 and 8, sintered grades 2,5,8; GM, Delco Remy Division which produces Nd–Fe–B, limited to several shapes only (Magnaquench), isotropic and anisotropic, many grades, under the name of Permag, in the form of disks, rectangles, and squares, supplied by the Magnetic Materials Division of the Dexter Corp.; Sumitomo,which produces Nd–Fe–B and sintered magnets; 3M Co., which produces magnetic oxides, ferrites rubber bonded to form flexible permanent magnet tape with or without adhesive (Plastiform); and AlliedSignal, which produces the amphorous magnetic alloys known as Metglas. Other manufacturers are listed in Tables 4 and 10.

BIBLIOGRAPHY

"Magnetic Substances" in *ECT* 1st ed., Vol. 8, pp. 639–659 by R. A. Chegwidden, Bell Telephone Laboratories, Inc.; "Magnetic Materials" in *ECT* 2nd ed., Vol. 12, pp. 737–772, by E. A. Nesbitt, Bell Telephone Laboratories; "Magnetic Materials, Bulk" in *ECT* 3rd ed., Vol. 14, pp. 646–686, by G. Y. Chin and J. H. Wernick, Bell Laboratories.

CITED PUBLICATIONS

1. *J. Appl. Phys.* **49**, 1599 (1978).
2. P. A. Beck, *Prog. Mater. Sci.* **23**, 1 (1978).
3. S. Chikazumi and C. D. Graham, Jr., in A. Berkowitz and E. Kneller, eds., *Magnetism and Metallurgy*, Vol. **2**, Academic Press, Inc., New York, 1969, "Chapt. 12".
4. G. Y. Chin, *Adv. Mater. Res.* **5**, 217 (1971).
5. L. H. Bennett, C. H. Page, and L. J. Swartzendruber, *AIP Conf. Proc.*, (29), xix (1976).
6. C. D. Graham, Jr., *IEEE Trans. Mag.* **12**, 822 (1977).
7. M. McCaig, *Permanent Magnets in Theory and Practice*, John Wiley & Sons, Inc., New York, 1977.
8. *IEC Publ.* **50**, 901 (1973).
9. C. Heck, *Magnetic Materials and Their Applications*, Crane, Russak & Co., Inc., New York, 1974, 23–35.
10. M. F. Littmann, *IEEE Trans. Mag.* **7**, 48 (1971).
11. J. W. Swisher, A. T. English, and R. C. Stoffers, *Trans. ASM* **62**, 257 (1969); J. H. Swisher and E. O. Fuchs, *J. Iron Steel Inst.*, 777 (Aug. 1970).
12. *Steels Products Manual—Flat Rolled Electrical Steel*, American Iron and Steel Institute (AISI), Washington, D.C., 1978.
13. Ref. 9, p. 317.
14. U.S. Pat. 1,965,559 (1934), N. P. Goss (to Cold Metal Process. Co.).
15. S. Taguchi, T. Yamamoto, and A. Sakakura, *IEEE Trans. Mag.* **10**, 123 (1974).

16. F. A. Malagari, *IEEE Trans. Mag.* **13**, 1437 (1977).
17. S. Taguchi, *Trans. ISIJ* **17**, 604 (1977).
18. G. Y. Chin and J. H. Wernick, in E. P. Wohlfarth, ed., *Ferromagnetic Materials*, Vol. **2**, North-Holland Publishing Co., New York, 1980, "Chapt. 2".
19. *Report E-172 (Tufperm)*, Hitachi Metals Ltd., Tokyo.
20. Ref. 18, p. 143.
21. F. Pfeifer and R. Cremer, *Z. Metall.* **64**, 362 (1973).
22. O. L. Boothby and R. M. Bozorth, *J. Appl. Phys.* **18**, 173 (1947).
23. F. Pfeifer, *Z. Angew. Phys.* **28**, 20 (1969).
24. F. Pfeifer and R. Boll, *IEEE Trans. Mag.* **5**, 365 (1969).
25. G. Y. Chin, T. C. Tisone, and W. B. Grupen, *J. Appl. Phys.* **42**, 1502 (1971).
26. H. L. B. Gould and D. H. Wenny, *AIEE Spec. Publ. T-97*, 675 (1957).
27. Ref. 18, pp. 175 and 179.
28. D. R. Thornburg, *J. Appl. Phys.* **40**, 1579 (1969).
29. B. Thomas, *Proceedings Conference Soft Magnetic Materials*, Cardiff, Wales, 1975, p. 109.
30. R. V. Major, M. C. Martin, and M. W. Branson, *Proceedings Conference Soft Magnetic Materials*, Cardiff, Wales, 1975, p. 103.
31. A. Beer and T. Schwartz, *IEEE Trans. Mag.* **2**, 470 (1966).
32. "Ferrite Cores—for Telecommunication and Industrial Fields," *TDK Data Book*, TDK Electronics Co., Ltd., Skokie, Ill., Feb. 1981.
33. C. H. Smith, *IEEE Trans. Mag.* **18**, 1376 (1982).
34. T. Akashi and co-workers, *Ferrites—Proceedings 1970 International Conference*, University of Tokyo Press, Japan, 1971, p. 183.
35. U.S. Pat. 3,609,083 (Sept. 28, 1971), P. I. Slick (to Bell Telephone Laboratories).
36. J. G. M. DeLau, *Philips Res. Rep. Suppl.*, (6) (1975).
37. P. I. Slick, in Ref. 18, Chapt. 3.
38. T. Inui and N. Ogasawara, *IEEE Trans. Mag.* **13**, 1729 (1977).
39. *Microwave Ferrite Specification Bulletin 1972–1979*, Trans-Tech, Inc., Gaithersberg, Md.
40. F. E. Luborsky and co-workers, *J. Appl. Phys.* **49**, 1769 (1978).
41. R. C. O'Handley, C.-P. Chou, and N. DeCristofaro, *Conference of Magnetics & Magnetic Materials*, Cleveland, Ohio, Nov. 1978; R. Hasegawa and R. C. O'Handley, *J. Appl. Phys.* **50** 1551 (1979).
42. S. Hatta, T. Egami, and C. D. Graham, Jr., *Appl. Phys. Lett.* **34**(1), 113 (1979).
43. *MMPA Standard 0100-78*, Magnetic Materials Producers Association, Evanston, Ill., 1978.
44. A. Hoffmann and P. Pant, *Tech. Mitt. Krupp. Forsch. Ber.* **28**, 117 (1970); *Tech. Mitt. Krupp. Fursch. Ber.* **33**, 25 (1975).
45. G. Y. Chin, J. T. Plewes, and B. C. Wonsiewicz, *J. Appl. Phys.* **49**, 2046 (1978); B. C. Wonsiewicz, J. T. Plewes, and G. Y. Chin, *IEEE Trans. Mag.* **15**, 950 (1979).
46. S. Jin, *IEEE Trans. Mag.* **15**, 1748 (1979).
47. M. L. Green and co-workers, *IEEE Trans. Mag.* **16**, 1053 (1980).
48. T. Ohtani and co-workers, *IEEE Trans. Mag.* **13**, 1328 (1977).
49. R. D. Heidenreich and E. A. Nesbitt, *J. Appl. Phys.* **23**, 352 (1952).
50. A. J. Luteijn and K. J. deVos, *Philips Res. Rep.* **11**, 489 (1956).
51. J. Harrison, *Z. Angew. Phys.* **21**, 101 (1966).
52. D. J. Palmer and S. W. K. Shaw, *Cobalt* **43**, 55 (1969).
53. P. Pant and H. Stablein, "Manufacture and Properties of Columnar Alnico Permanent Magnets," presented at the *World Electrotechnical Congress*, Moscow, Russia, June 21–25, 1977.
54. A. Cochardt, *J. Appl. Phys.* **37**, 1112 (1966).

55. E. A. Nesbitt, J. H. Wernick, and E. Corenzwit, *J. Appl. Phys.* **30**, 365 (1959); E. A. Nesbitt and co-workers, *J. Appl. Phys.* **32**, 342 (1961).
56. K. N. R. Taylor, *Adv. Phys.* **20**, 551 (1971).
57. A. Menth, H. Nagel, and R. S. Perkins, *Ann. Rev. Mater. Sci.* **8**, 21 (1978).
58. K. Strnat and co-workers, *J. Appl. Phys.* **37**, 1252 (1966).
59. E. A. Nesbitt and J. H. Wernick, *Rare Earth Permanent Magnets*, Academic Press, Inc., New York, 1973.
60. W. E. Wallace, *Rare Earth Intermetallics*, Academic Press, Inc., New York, 1973.
61. T. Ojima and co-workers, *Jpn. J. Appl. Phys.* **16**, 671 (1977); *IEEE Trans. Mag.* **13**, 1317 (1977); K. J. Strnat, ed., *Proceedings 3rd International Workshop on Rare Earth-Cobalt Permanent Magnets*, University of Dayton, Ohio, 1978, p. 406.
62. K. J. Strnat, in *Proceedings 4th International Workshop on Rare Earth-Cobalt Permanent Magnets*, Society Non-Traditional Technology, Tokyo, 1979, p. 8.
63. J. J. Croat and co-workers, *Appl. Phys. Lett.* **44**, 148 (1984).
64. D. J. Sellmyer and co-workers, *J. Appl. Physics* **55**, 2088 (1984).
65. M. Sagawa and co-workers, *Jpn. J. Appl. Phys.* **26**, 785 (1987).
66. K. J. Strnat, in E. P. Wohlfarth and K. H.-J. Buschow, eds., *Ferromagnetic Materials*, Vol. **4**, Elsevier, Amsterdam, 1988.
67. K. H.-J. Buschow, *Rep. Prog. Phys.* **54**, 1123 (1991).
68. J. F. Herbst and co-workers, *Phys. Rev.* **B29**, 4176 (1984).
69. D. Givord, H. S. Li, and J. M. Moreau, *Solid State Commun.* **50**, 497 (1984).
70. J. M. D. Coey and H. Sun, *J. Magn. and Magn. Mat.* **87**, L251 (1990).
71. Y. Otani and co-workers, *J. Appl. Phys.* **69**(8), 5584 (1991).
72. H. H. Stadelmaier and E. T. Henig, *JOM* **43**(2), 32 (1991); *J. Mat. Eng. Perform.* **1**(2), 167 (1992).
73. J. J. Croat and J. F. Herbst, *MRS Bulletin*, 37 (June 1988).
74. J. D. Livingston, in Jan Evetts, ed., *Concise Encyclopedia of Magnetic and Superconducting Materials*, Pergamon Press Inc., Elmsford, N.Y., 1992, p. 344.
75. K. Raja and co-workers, *J. Appl. Phys.* **73**, 967 (1993).
76. M. Leonowicz and H. A. Davies, *Mat. Lett.* **19**, 275 (1994).
77. K. H.-J. Buschow, in Ref. 74.
78. D. Howe and T. S. Birch, in G. J. Long and F. Grandjean, eds., *Supermagnets, Hard Magnetic Materials*, Kluwer Dordrecht, the Netherlands, 1990, p. 679.
79. H. Kaneko, M. Homma, and K. Nakamura, *AIP Conf. Proc.* **5**, 1088 (1971).
80. G. Y. Chin, *J. Magn. Mag. Mat.* **9**, 283 (1978).
81. H. Zijlstra, *IEEE Trans. Magn.* **14**, 661 (1978).
82. S. Jin, *IEEE Trans. Magn.* **15**, 1748 (1979).
83. S. Jin, N. V. Gayle, and J. E. Bernardini, *IEEE Trans. Magn.* **16**, 1050 (1980).
84. M. L. Green and co-workers, *IEEE Trans. Magn.* **16**, 1053 (1980).
85. S. Jin and G. Y. Chin, *IEEE Trans. Magn.* **23**, 3187 (1987).
86. S. Jin, G. Y. Chin, and B. C. Wonsiewicz, *IEEE Trans. Magn.* **16**, 139 (1980).
87. T. Ohtani and co-workers, *IEEE Trans. Magn.* **13**, 1328 (1977).
88. M. R. Pinnel, *IEEE Trans. Magn.* **12**, 789 (1976).

GENERAL REFERENCES

R. Ball, *Soft Magnetic Materials*, Heyden and Sun Ltd., London, 1979, handbook of soft magnetic materials.
R. M. Bozorth, *Ferromagnetism*, 5th printing, D. Van Nostrand Co., Princeton, N.J., 1951; reprinted by IEEE.

M. McCaig, *Permanent Magnets in Theory and Practice*, John Wiley & Sons, Inc., New York, 1977.
E. P. Wolfarth, ed., *Ferromagnetic Materials—A Handbook on the Properties of Magnetically Ordered Substances*, Vols. **1** and **2**, Elsevier, New York 1980; E. P. Wolfarth and K. H.-J. Buschow, eds., Vols. **3** and **4**, Elsevier, 1988.
C. W. Chen, *Magnetism and Metallurgy of Soft Magnetic Materials*, North-Holland, New York, 1977.
C. Heck, *Magnetic Materials and Their Applications*, Crane, Russak and Co., Inc., New York, 1974.
F. E. Luborsky, ed., *Amorphous Metallic Alloys*, Butterworths, London, 1983.
T. R. Anantharaman, *Metallic Glasses: Production, Properties and Applications*, Trans. Tech. Publications, Switzerland, 1983.
J. F. Herbst, "Permanent Magnets," *Am. Sci.*, 251 (May–June 1993).

JACK WERNICK
Bell Telephone Laboratories, Inc.

Table 1. **Magnetic Properties of Fully Annealed Iron and Iron Alloys**[a]

Iron and alloys	B_s, T[b]	Density, g/cm^3	Resistivity, μΩ·cm	H_c (B_m = 1 T),[b] A/cm[d]	Permeability, A/cd[d]		Core loss (1.5 T,[b] 60 Hz), W/kg[c]		
					$H = 0.8$	$H = 8$	0.35 mm	0.46 mm	0.64 mm
magnetic ingot iron									
cast	2.15	7.85	10.7	0.68	3,500	1,500			
0.2-cm sheet	2.15	7.85	10.7	0.88	1,800	1,575			13.20
electromagnet iron, 0.2-cm sheet	2.15	7.85	12.0	0.81	2,750	1,575			
hydrogen-annealed iron	2.15	7.85	10.1	0.04	14,000	1,580			
low carbon steel, decarburized	2.14	7.85	12.5	0.70	2,000	1,530	8.10	9.2	11.44
cold-rolled									
M36 Si–Fe	2.04	7.75	41.0	0.36	7,400	1,485		3.85	4.73
M22 Si–Fe	1.98	7.65	49.0	0.31	8,100	1,450		3.63	4.29
M6 (110)[001] 3.2% Si–Fe	2.03	7.65	48.0	0.06	16,000	1,820	1.45		

[a]Ref. 10.
[b]To convert T to G, multiply by 10^4.
[c]At thickness shown.
[d]To convert A/cm to Oe, divide by 0.7958.

Table 2. **Core Loss of Grain-Oriented Silicon Steels, W/kg**[a]

	0.27 mm		0.30 mm		0.35 mm	
Grade	50 Hz	60 Hz[b]	50 Hz[c]	60 Hz	50 Hz[c]	60 Hz
			High induction			
M0H	(0.99)	1.32	1.05	(1.41)		
M1H	(1.04)	1.40	1.11	(1.49)	1.16	(1.55)
M2H	(1.11)	1.49	1.17	(1.56)	1.22	(1.63)
M3H	(1.17)	1.57	1.23	(1.65)	1.28	(1.72)
M4H					1.37	(1.84)
			Conventional			
M4(27H076)[d]	1.27	1.67				
	0.89[e]	1.17[e]				
M5(30H083)[d]			1.39	1.83		
			0.97[e]	1.28[e]		
M6(35H094)[d]					1.57	2.07
					1.11[e]	1.45[e]

[a]At 1.7 T (1.7×10^4 G) unless otherwise noted. Data in parentheses calculated on basis of loss (60 Hz)/loss (50 Hz) = 1.34 typical of high induction material.
[b]Data for 0.28-mm thick samples; Ref. 16.
[c]Ref. 17.
[d]ASTM A725-75.
[e]Core loss at 1.5 T (1.5×10^4 G).

Table 3. **Properties of Materials Intended for Recording-Head Applications**[a]

Property	4-79 Permalloy[b]	Tufperm[c]		16% Al–Fe	Sendust	Ferrite
		YEP-H	YEP-S			
hardness, Vickers', H_V	120	230	290	290	480	580
μ, at 1 kHz, 0.2 mm	11,000	11,000	7,000	4,000	8,000	4,500
ρ, $\mu\Omega \cdot$ cm	100	60	100	150	85	10^6–10^7
B_s, T[d]	0.8	0.5	0.5	0.8	1.0	0.4
H_c, A/cm[e]	0.02	0.01	0.02	0.03	0.02	0.06
T_C, °C	460	280	280	350	500	150

[a]Ref. 19.
[b]CAS Registry Number [39323-53-0].
[c]Ti–Nb–Mo Permalloy, Hitachi Magnetic Metals Designation.
[d]To convert T to G, multiply by 10^4.
[e]To convert A/cm to Oe, divide by 0.7958.

Table 4. **Materials for Laminations, Cut-Cores, and Tape-Wound Cores**[a]

Alloy type	Trade names[b]	μ_i, $\mu_0 \times 10^{-3}$	μ_m, $\mu_0 \times 10^{-3}$	H_c, A/cm[c]	B_s, T[d]	B_r, T[d]	$\frac{B_r}{B_m}$	T_C, °C	Resistivity, μΩ·cm	Density, g/cm^3
			High initial μ							
36Ni	Permenorm 3601 K2, Hyperm 36M, Radiometal 36, 0.3 mm/50 Hz	3	20	0.16	1.3			250	75	8.15
48Ni	4750 Alloy, High Permeability 49, Hyperm 52, Alloy 48, Superperm 49, Super Radiometal, Permenorm 5000 H2, 0.15 mm/60 Hz	11	80	0.024	1.55			480	48	8.25
56Ni	Permax M, 0.15 mm/60 Hz	30	125	0.016	1.5			500	45	8.25
4Mo–80Ni	4-79Mo–Permalloy, HyMu 80, Round Permalloy 80, Superperm 80, 0.1 mm/60 Hz	40	200	0.012	0.8			460	58	8.74
4Mo–5Cu–77Ni	Mumetal Plus, Hyperm 900, Vacoperm 100, 0.1 mm/60 Hz	40	200	0.012	0.8			400	58	8.74
			High initial μ							
5Mo–80Ni	Supermalloy, HyMu 800, Hyperm Maximum, 0.1 mm/60 Hz	70	300	0.004	0.78			400	65	8.77
4Mo–5Cu–77Ni	Supermumetal, Ultraperm 10, 0.1 mm/60 Hz	70	300	0.004	0.8			400	60	8.74
			Square loop							
4Mo–80Ni	Square Permalloy, HyRa 80, Square Permalloy 80, Square 80, 0.05 mm/(0.4 A/cm) dc			0.024	0.8	0.66	0.80	460	58	8.74
4Mo–5Cu–77Ni	Ultraperm Z, Orthomumetal, 0.015 mm/(0.4 A/cm) dc			0.024	0.8	0.66	0.80	400	58	8.74
3Mo–65Ni	Permax Z, 0.05 mm/(0.4 A/cm) dc			0.02	1.25	1.05	0.94	520	60	8.50
50Ni	Deltamax, HyRa 49, Hyperm 50T, Orthonol, Square 50, HCR Alloy, Permenorm Z, 0.05 mm/(0.4 A/cm) dc			0.08	1.60	1.50	0.95	500	45	8.25

		Square loop						
3Si	Silectron, Microsil, Magnesil, Hyperm 5T/7T, 0.1 mm/ (2.4 A/cm) dc	0.32	2.03	1.63	0.85	730	50	7.65
2V–49Co	Supermendur, Vaco-flux Z, Hyperm Co50, 0.1 mm/ (2.4 A/cm) dc	0.16	2.30	2.00	0.90	940	26	8.15
		Skewed (flat) loop						
4Mo–5Cu–77Ni	Ultraperm F	0.012	0.8	0.12		400	58	8.74
3Mo–65Ni	Permax F	0.10	1.25	0.15		520	60	8.50

[a]Ref. 20.

[b]Manufacturers for alloys: Arnold Engineering: 4-79 Mo Permalloy, Supermalloy, Square Permalloy, Supermendur, Deltamax, Silectron, 4750 alloy. Carpenter Technology: HyMu80, HyMu800, High Permeability 49, HyRa49, HyRa80. F. Krupp Widiafabrik: Hyperm 36M, Hyperm 52, Hyperm 50T, Hyperm 5T/7T, Hyperm 900, Hyperm Maximum, Hyperm Co50. Magnetics, Division of Spang, Inc.: Alloy 48, Round Permalloy 80, Square Permalloy 80, Orthonol, Supermendur, Magnesil. Magnetic Metals: Superperm 49, Superperm 80, Square 80, Square 50, Microsil. Telcon Metals: Radiometal 36, Superradiometal, Mumetal Plus, Supermumetal, HCR alloy, Orthomumetal. Vacuumschmelze: Permenorm 3601 K2, Permenorm 500 H2, Permenorm Z, Permax F, Permax M, Permax Z, Vacoperm 100, Ultraperm 10, Ultraperm F, Ultraperm Z, Vacoflex Z.

[c]To convert A/cm to Oe, divide by 0.7958.

[d]To convert T to G, multiply by 10^4.

Table 5. **Properties of Co–Fe Alloys**[a]

Property	Hiperco 27	Hiperco 35	2V Permendur	Supermendur
composition	27Co–0.5Cr–Fe	35Co–0.5Cr–Fe	2V–49Co–49Fe	2V–49Co–49Fe
electrical resistivity, $\mu\Omega \cdot$ cm	19	40	25	25
induction, T[b]				
saturation	2.36	2.4	2.4	2.4
remanent	1.0		1.5	2.2
μ_m, μ_0	2,800		8,000	92,500
H_c, A/cm[c]	2.0	2.0	4	0.16

[a]Ref. 27.
[b]To convert T to G, multiply by 10^4.
[c]To convert A/cm to Oe, divide by 0.7958.

Table 6. **Characteristics of Ferrites**[a]

Property	MnZn ferrites					
code[a]	H5A	H5B	H5C2	H5E	H6F	H6H3
practical frequency, MHz	<0.2	<0.1	<0.1	<0.01	0.2–2.0	0.01–0.8
initial permeability, μ_o	3,300	5,000	10,000	18,000	800	1,300
relative loss factor, tan $\delta/\mu_i \times 10^6$, at (kHz)	<2.5 (10)	<6.5 (10)	<7.0 (10)		<17 (1,000)	<1.2 (100)
temperature coefficient of $\mu_i \times 10^6$ from -30 to 20°C, $(\mu_2 - \mu_1)/\mu^2{}_1(T_2 - T_1)$	−0.5 to 2.0	−0.5 to 2.0	−0.5 to 1.5	−0.5 to 2.0		0.3 to 2.0
Curie temperature, °C	>130	>130	>120	>115	>200	>200
saturation flux density, T[b]	0.41	0.42	0.40	0.44	0.40	0.47
disaccommodation factor, $D \times 10^6$ (from 1–10 min), $(\mu_1 - \mu_2)/\mu^2{}_1\log(t_2/t_1)$ where t = time	<3	<3	<1	<1	<12	<5
resistivity, Ω·m	1	1	0.15	0.05	4	25
applications			transformers			inductors

Property	MnZn ferrites			NiZn ferrites		
code[a]	H6K	H7C1	H7C2	K5	K6A	K8
practical frequency, MHz	0.01–0.3	<0.3	<0.2	<8	1–50	<200
initial permeability, μ_o	2,200	2,500	3,900	290	25	16
relative loss factor, tan $\delta/\mu_i \times 10^6$, at (kHz)	<3.5 (100)			<28 (1,000)	<150 (10,000)	<250 (100,000)
temperature coefficient of $\mu_i \times 10^6$ from -30 to 20°C, $(\mu_2 - \mu_1)/\mu^2{}_1(T_2 - T_1)$	0.4 to 1.2			−4.0 to 2.0		
Curie temperature, °C	>130	>230	>200	>280	>450	>500
saturation flux density, T[b]	0.39	0.51	0.48	0.33	0.30	0.27
disaccommodation factor, $D \times 10^6$ (from 1–10 min), $(\mu_1 - \mu_2)/\mu^2{}_1\log(t_2/t_1)$ where t = time	<2			<30	<20	
resistivity, Ω·m	8	10	2	20×10^5	2.5×10^5	1.0×10^5
applications			power supplies		inductors	Inductors

[a]Ref. 32.

[b]To convert T to G, multiply by 10^4.

Table 7. **Selected Microwave Materials**[a]

Material	J_s, T[b]	ΔH, A/cm[c]	ϵ'	Loss tangent (tan δ)	T_C, °C	Remarks
			Garnets			
Y	0.180	36	15.0	2×10^{-4}	280	
YAl	0.018	36	13.8	2×10^{-4}	105	decreasing aluminum content
YAl	0.120	36	14.8	2×10^{-4}	220	
YGd	0.073	160	15.4	2×10^{-4}	280	decreasing Gd, low $\Delta M_s/\Delta T$,
YGd	0.160	40	15.1	2×10^{-4}	280	constant T_c
YGdAl	0.040	52	14.2	2×10^{-4}	150	similar to YAl, but lower
YGdAl	0.140	40	15.1	2×10^{-4}	265	$\Delta M_s/\Delta T$,
			Spinels			
MgMnAl	0.075	96	11.3	2.5×10^{-4}	90	decreasing aluminum content
MgMnAl	0.175	180	12.2	2.5×10^{-4}	225	
MgMn	0.215	432	12.7	2.5×10^{-4}	320	
MgMnZn	0.250	416	12.9	2.5×10^{-4}	275	increasing zinc content
MgMnZn	0.280	432	13.1	2.5×10^{-4}	225	
NiZn	0.400	272	12.3	2.5×10^{-3}	470	high J_s
NiZn	0.500	128	12.5	1.0×10^{-3}	375	high J_s
Li	0.375	520	15.0	2.5×10^{-3}	640	high T_c
LiZn	0.480	192	14.5	2.5×10^{-3}	400	high J_s
LiTi	0.100	240	18.0	2.5×10^{-3}	300	decreasing titanium
LiTi	0.290	440	15.2	2.5×10^{-3}	600	content

[a] Ref. 39.
[b] To convert T to G, multiply by 10^4.
[c] To convert A/cm to Oe, divide by 0.7958.

Table 8. **Properties of Amorphous Magnetic Alloys**[a]

Alloy	Composition	Saturation induction, B_s, T[b]	Coercive force H_c, A/m	Magnetostriction, $\lambda_s \times 10^{-6}$	Resistivity, ρ, $\mu\Omega \cdot$ cm	T_C, °C	Core loss: 60 Hz, 1.4 T,[b] W/kg	Core loss: 20 kHz, 0.2 T,[b] kW/m^3
			Iron-based					
Metglas 2605SC	$Fe_{81}B_{13.5}Si_{3.5}C_2$	1.61	3.2	30	1.30	370	0.3	300
Metglas 2605S-2	$Fe_{78}B_{13}Si_9$	1.56	2.4	27	1.30	415	0.23	
Metglas 2605CO	$Fe_{67}Co_{18}B_{14}Si_1$	1.80	4.0	35	1.30	415	0.55	
Metglas 2605S-3	$Fe_{79}B_{16}Si_5$	1.58	8.0	27	1.25	405	1.2	58
			Iron–nickel-based					
Metglas 2826MB	$Fe_{40}Ni_{38}Mo_4B_{18}$	0.88	1.2	12	1.60	353		200
			Cobalt-based					
Metglas 2705M	$Co_{67}Ni_3Fe_{4-}Mo_2B_{12}Si_{12}$	0.72	0.4	0.5	1.35	340		43

[a]Refs. 33 and 40.
[b]To convert T to G, multiply by 10^4.

Table 9. **Magnetic Properties of Commercial Permanent Magnet Materials Ferroxdure**

Material	T_C, °C	$(BH)_{max}$, kJ/m^3[a]	B_r, T[b]	H_c, kA/m[c]
Ferroxdure ($SrFe_{12}O_{19}$)	450	36	0.42	250
Alnico 9	850	72	1.05	120
$SmCo_5$	724	144	0.87	600
$Sm(Co_{0.68}Cu_{0.10}Fe_{0.21}Zr_{0.01})_{7.4}$	800	240	1.10	510
$Nd_2Fe_{14}B$	312	290	1.23	880

[a]To convert kJ/m^3 to G·Oe, multiply by 12.57×10^4.
[b]To convert T to G, multiply by 1×10^4.
[c]To convert kA/m to Oe, divide by 7.958×10^{-2}.

Table 10. **Properties of Permanent (Hard) Magnet Materials**[a]

Magnet material	Chemical composition	B_r, T[b]	H_c, kA/m[c]	$(BH)_{max}$, kJ/m^3[d]
$3\frac{1}{2}$% Cr steel	3.5Cr,1C,bal Fe	1.03	5	2.4
3% Co steel	3.25Co,4Cr,1C,bal Fe	0.97	6	3.0
17% Co steel	18.5Co,3.75Cr,5W,0.75C,bal Fe	1.07	13	5.5
36% Co steel	38Co,3.8Cr,5W,0.75C,bal Fe	1.04	18	7.8
Alnico 1	12Al,21Ni,5Co,3Cu,bal Fe	0.72	37	11.0
Alnico 2	10Al,19Ni,13Co,3Cu,bal Fe	0.75	45	13.5
Alnico 4	12Al,27Ni,5Co,bal Fe	0.56	57	10.7
Alnico 5 DG[e]	8Al,14Ni,24Co,3Cu,bal Fe	1.33	53	52.0
Alnico 5 Col.[e]	8Al,14Ni,24Co,3Cu,bal Fe	1.35	59	60.0
Alnico 8[e]	7Al,15Ni,35Co,4Cu,5Ti,bal Fe	0.82	130	42.0
Alnico 9[e]	7Al,15Ni,35Co,4Cu,5Ti,bal Fe	1.05	120	72.0
Col. Alnico HC[e,f]	7Al,14Ni,40Co,3Cu,7.5Ti,bal Fe	0.97	150/155[g]	91.5
Col. Alnico HC[e,f]	7Al,14Ni,39Co,3Cu,8Ti,bal Fe	0.88	170/180[g]	77.0
sintered Alnico 6[e]	8Al,16Ni,24Co,3Cu,1Ti,bal Fe	0.94	63	23.0
sintered Alnico 8 HC[e]	7Al,14Ni,38Co,3Cu,8Ti,bal Fe	0.67	140	36.0
Ceramic 7[e,h]	$MO6Fe_2O_3$	0.34	260/320[g]	22.0
bonded ceramic[e,i]	flexible anisotropic ferrite	0.24	170/215[g]	11.0
Cunife 1[e]	60Cu,20Ni,20Fe	0.55	42	11.0
Vicalloy 1	10V,52Co,bal Fe	0.75	20	6.4
Remalloy	12Co,15Mo,bal Fe	0.97	20	8.0
rare-earth cobalt[e,j]	25.5Sm,8Cu,15Fe,1.5Zr,50Co	1.10	510/520[g]	240.0
Cr–Co–Fe[e,k]	23Co,31Cr,1Si,bal Fe	1.25	52	40.0
Cr–Co–Fe[e,l]	11.5Co,33Cr,bal Fe	1.20	60	42.0
Cr–Co–Fe[e,m]	5Co,30Cr,bal Fe	1.34	42	42.0

[a]All data adapted from Ref. 43 except where noted.
[b]To convert T to G, multiply by 10^4.
[c]To convert kA/m to Oe, divide by 7.958×10^{-2}.
[d]To convert kJ/m^3 to G·Oe, multiply by 12.57×10^4.
[e]Anisotropic.
[f]Ref. 44.
[g]Intrinsic coercive force, H_{cJ}.
[h]M represents Ba or Sr.
[i]TDK BQ A14 Rubber Magnet.
[j]TDK REC-30.
[k]Sumitomo CKS500.
[l]Chromidur III; Ref. 46.
[m]Ref. 47.

Table 11. **Magnetic Properties of RCo_5 and R_2Co_{17} Compounds**

R	CAS Registry number	J_s, T[a]	T_C, °C[b]	K_1, MJ/m^3[c]–[ed]
		RCo_5		
Ce	[12214-13-0]	0.85[f]	374	5.3
Pr	[12017-67-3]	1.12[f]	612	8.1
Nd	[12017-65-1]	1.20[f]	630	0.7
Sm	[12017-68-4]	0.97	724	17.2
		R_2Co_{17}		
Ce	[12014-88-9]	1.15[g]	800	−0.6
Pr	[12052-77-6]	1.38[g]	890	−0.6
Nd	[12052-76-5]	1.39[g]	900	−1.1
Sm	[12052-78-7]	1.20[g]	920	3.3

[a]To convert T to G, multiply by 10^4.
[b]Ref. 56.
[c]Values at 25°C.
[d]To convert MJ/m^3 to G·Oe, multiply by 12.57×10^7.
[e]Ref. 57.
[f]Ref. 55.
[g]Ref. 58.

Table 12. **Intrinsic Properties of Ternary R-Based Magnetic Materials**[a]

Material	Curie temperature, T_C, °C	M_s, T[b]	Anisotropy field, H_a, MA/m[c]	$(BH)^{th}_{max}$, kJ/m^3[d]
$Nd_2Fe_{14}B$	312	1.60	5.4	512
$Nd_2Fe_{14}C$	262	1.50	7.6	450
Fe_3B:Nd	512	1.60		512
$SmFe_{11}Ti$	312	1.16	7.4	268
$SmFe_{10}V_2$	337	1.10	4.8	240
$SmFe_{10}Mo_2$	187	0.97	>4.0	188
$Sm_2Fe_{17}C$	267	1.42	4.2	403
$Sm_2Fe_{17}N_{2.7}$	477	1.50	11.2	450
$SmCo_5$	747	1.14	24	258
$Sm(Co,Fe,Cu)_7$	827	1.3	4.0	336
$Nd_2Co_{14}B$	722	1.15	8.0	266

[a]Ref. 67.
[b]To convert T to G, multiply by 1×10^4.
[c]To convert MA/m to kOe, multiply by 12.407.
[d]To convert kJ/m^3 to MG·Oe, multiply by 0.125.

Table 13. **Alloys for Application in Reed Contacts**[a]

Alloy	Coercive force, A/cm[b]	Remanent induction, T[c]	Squareness ratio	Magnetostrictive coefficient $\times 10^6$
49Co − 48Fe + 3V (Remendur)	24	1.8	0.90	50
38Co–39Fe–20Ni–3Nb	24	1.6	0.95	∼45
Co–Fe–Ni–Al–Ti (Vacozet 655)	32	1.4	0.90	48
85Co–12Fe–3Nb (Nibcolloy)	16	1.5	0.95	2
82Co–13Fe–5Mo	24	1.3	0.92	>0
84Co–12Fe–4Ti	18	1.4	>0.90	>0
82Co–12Fe–6Au	11	1.6	0.85	small
89Co–10Fe–1Be	24		0.90	small
54Fe–28Ni–18Co (Kovar)	<8	1.8	<0.70	
80Fe–16Ni–3Al–1Ti	24	1.3	0.90	0.4
76Fe–16Ni–5Cu–1W	28	1.4	0.95	
80Fe–18Cu–2Mn	24	1.5	0.90	

[a]Adapted from Ref. 85.
[b]To convert A/cm to Oe, divide by 0.7958.
[c]To convert T to G, multiply by 10^4.
[d]G = good; P = poor.

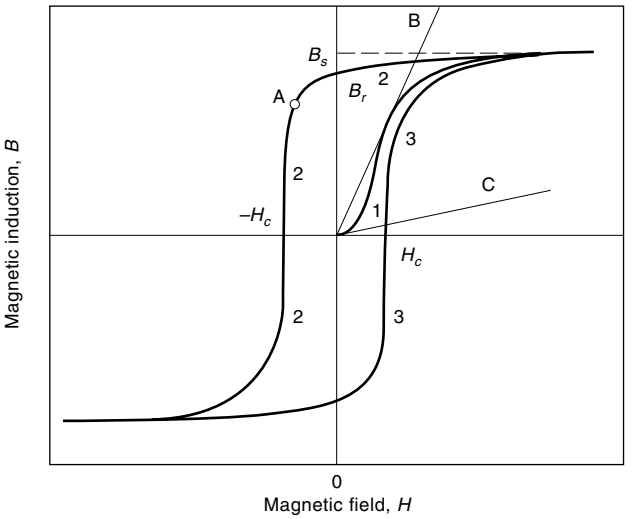

Fig. 1. Magnetic hysteresis loop of an initially demagnetized material (curve 1) where point A corresponds to $(BH)_{max}$; and the slopes of lines B and C, with tangents to curves 1 and 2, represent $\mu_m = B/H$ and μ_i, respectively. Terms are defined in the text.

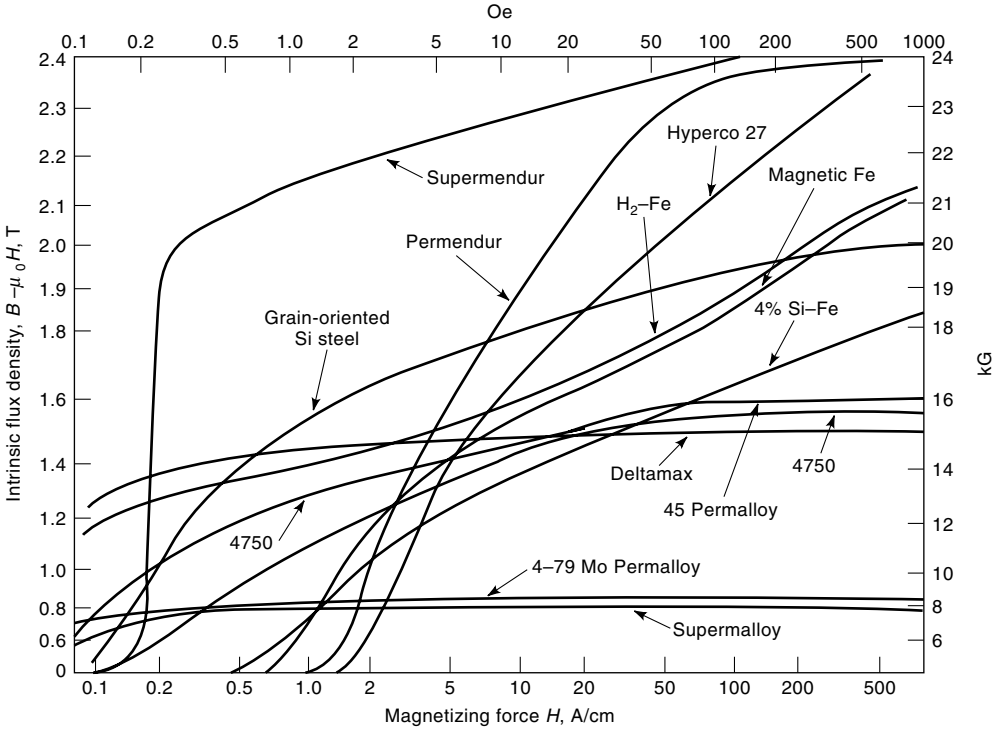

Fig. 2. Magnetization curves of commercial soft magnetic materials.

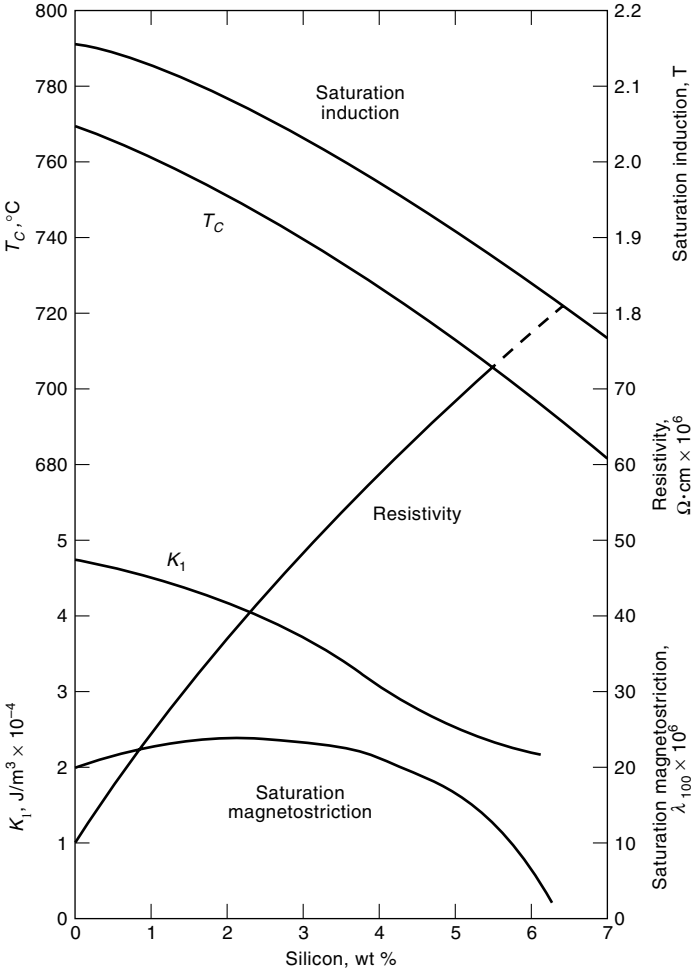

Fig. 3. Effect of silicon on properties of iron (10). T_C = Curie temperature; K_1 = magnetocrystalline anisotropy constant. To convert T to G, multiply by 10^4; to convert J/m^3 to erg/cm^3, multiply by 10.

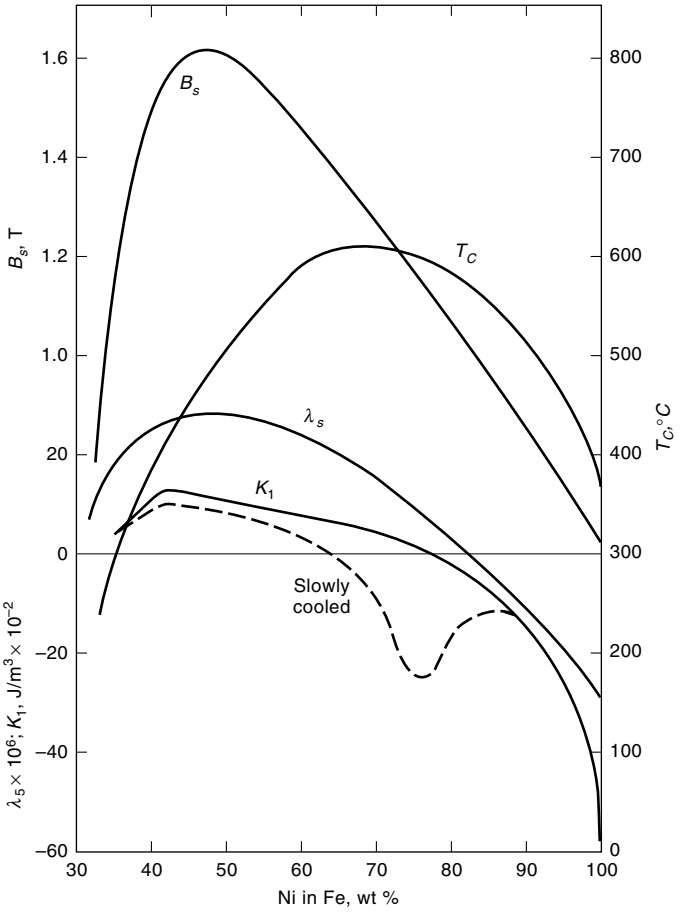

Fig. 4. Magnetic parameters of Ni–Fe alloys. To convert T to G, multiply by 10^4; to convert J/m^3 to erg/cm^3, multiply by 10.

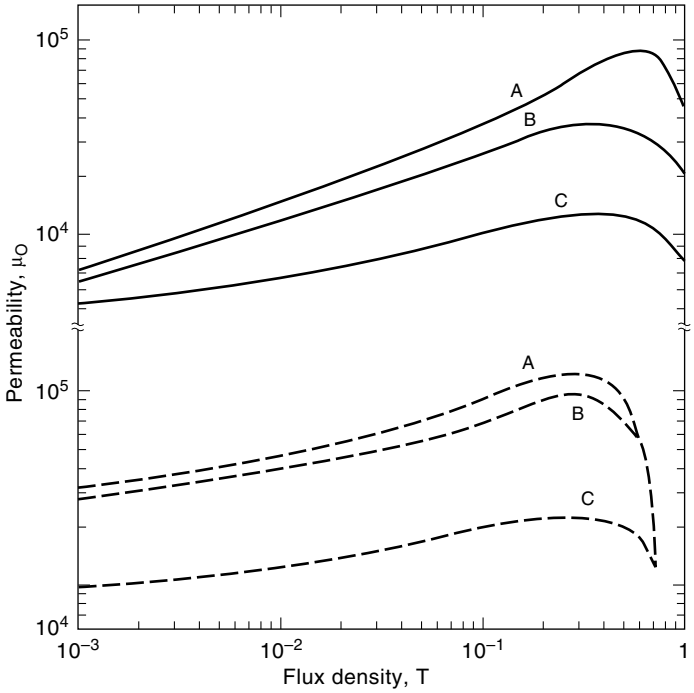

Fig. 5. Permeability-flux density curves for (—) Alloy 48, 0.35 mm (48% Ni) and (–) Permalloy 80, 0.35 mm (4 Mo, 80 Ni) where A represents dc; B, 60 Hz; and C, 400 Hz. To convert T to G, multiply by 10^4.

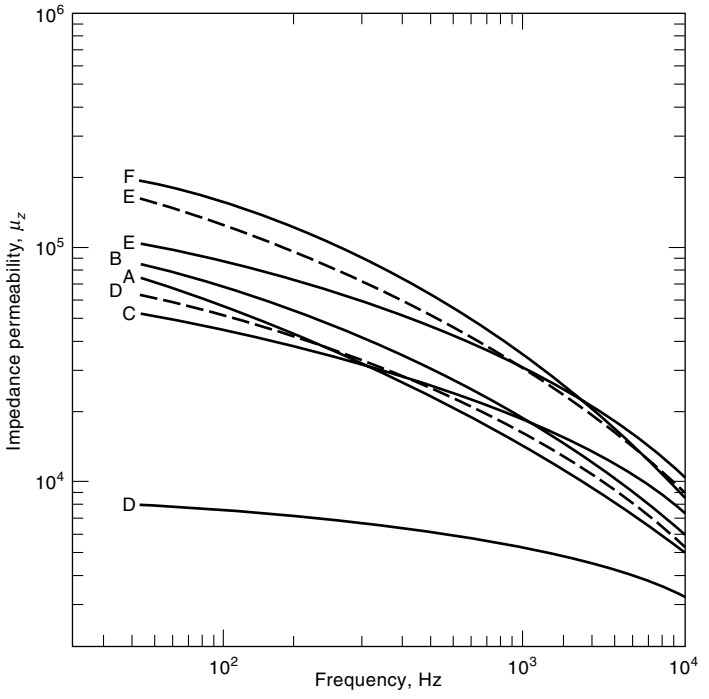

Fig. 6. Permeability-frequency curves of commercial thin-gauge tapes (0.1-mm thick) where A = Supermendur, 20 T; B = Magnesil, 1.0 T; C = Orthonol, 1.0 T; D = Alloy 48, (—) 0.004 T and (–) 1.0 T; E = Supermalloy, (—) 0.002 T and (–) 0.15 T; F = Sq permalloy 80, 0.60 T. To convert T to G, multiply by 10^4.

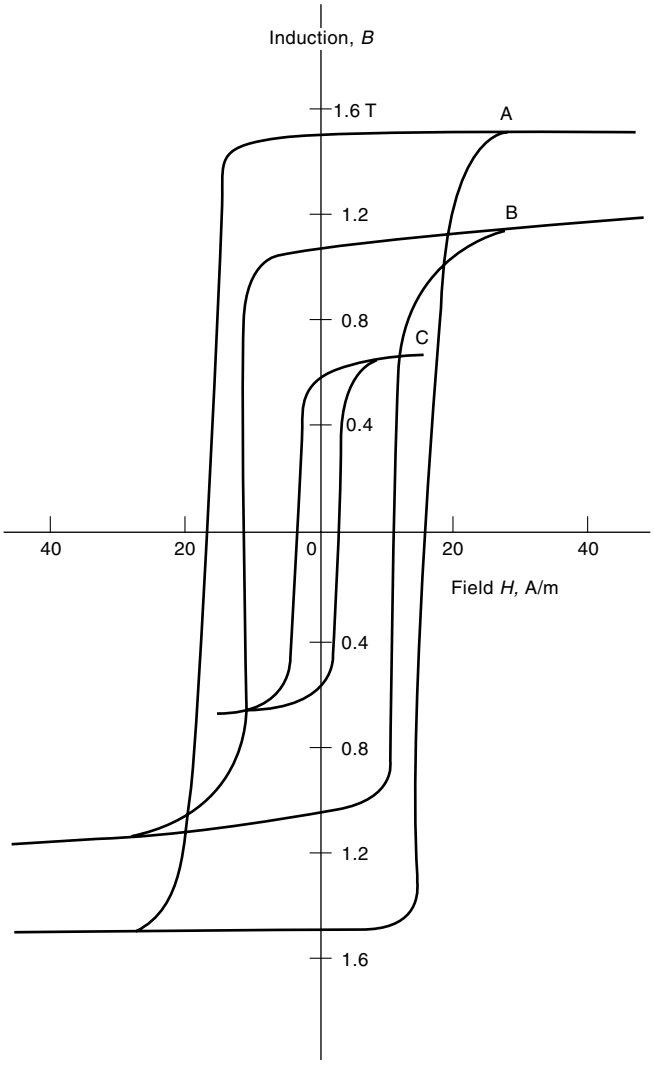

Fig. 7. Hysteresis loops at 60 Hz of three commercial Ni–Fe alloys: A, Orthonol; B, Alloy 48; and C, Permalloy 80. To convert A/m to Oe, divide by 79.58.

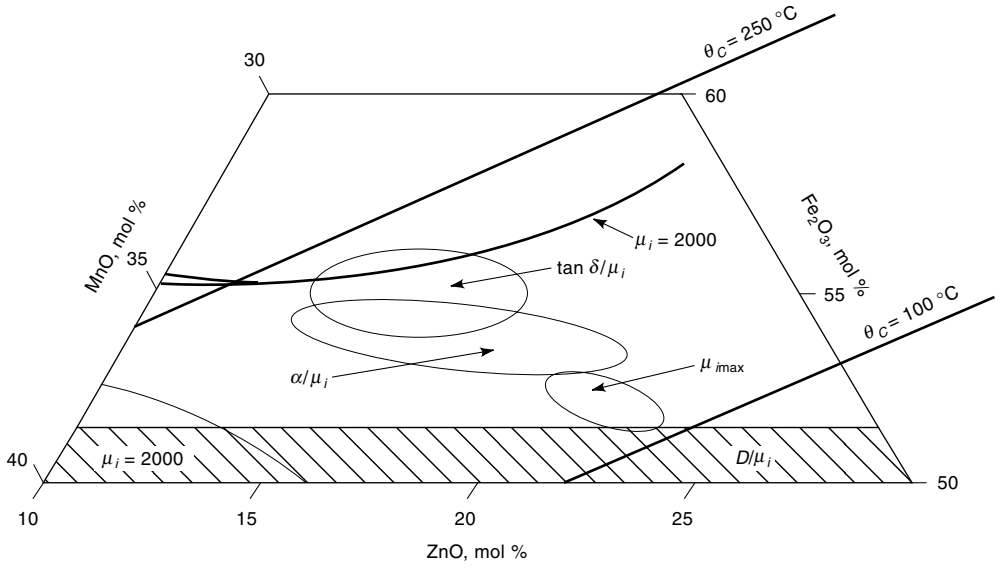

Fig. 8. Composition regions of optimal magnetic properties in the MnZn ferrite system (33). Values of μ_i in units of μ_0.

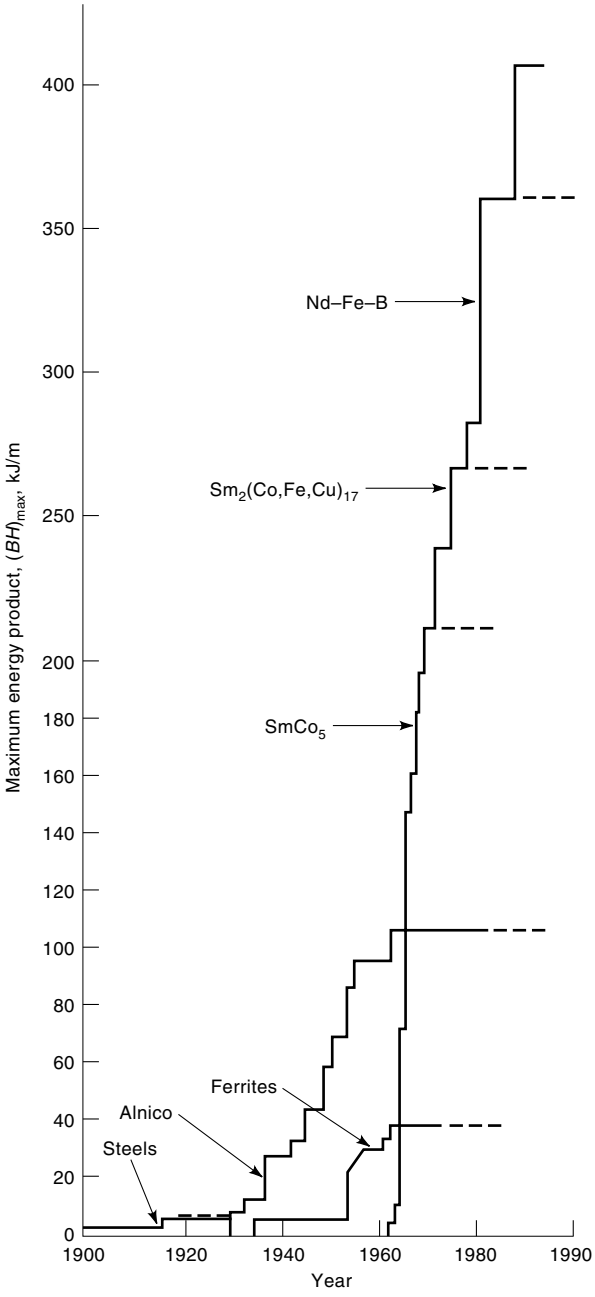

Fig. 9. Progress in energy product for hard magnetic materials. To convert J to cal, divide by 4.184.

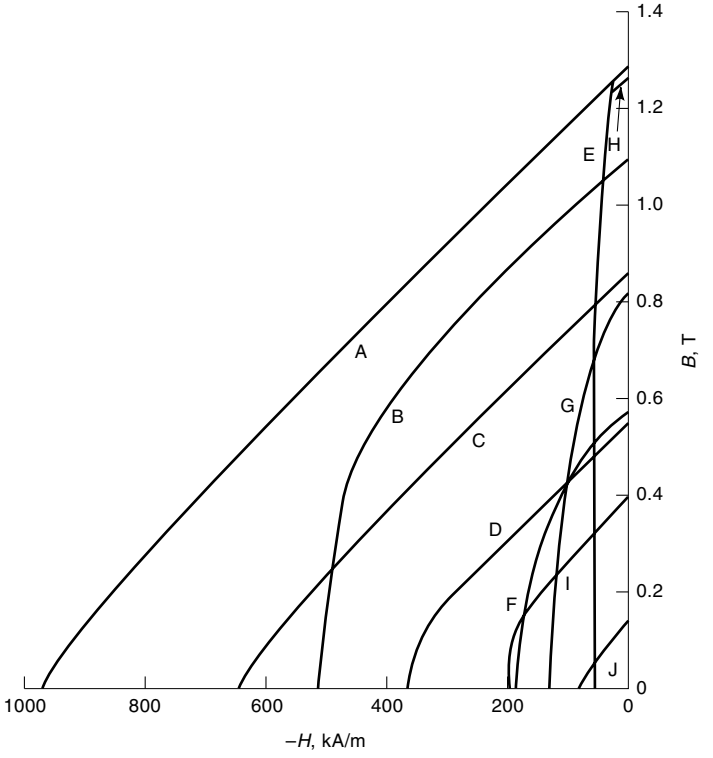

Fig. 10. Demagnetization curves of hard magnetic materials: A, $Nd_2Fe_{14}B$; B, $Sm(Co, Cu,Fe,Zr)_{7.4}$; C, $SmCo_5$; D, bonded $SmCo_5$; E, Alnico 5; F, Mn–Al–C; G, Alnico 8; H, Cr–Co–Fe; I, ferrite; J, bonded ferrite. To convert T to G, multiply by 10^4.